

**Rag Layer Formation and Stability of Crude Oil Emulsion Under Different  
Imposed Mechanical Energy and Temperatures**

**by**

**RACHAEL TAN FERN FERN  
14858**

**Dissertation submitted in partial fulfillment of the requirements for the  
Bachelor of Engineering (Hons)  
(Mechanical)**

**JANUARY 2015**

**Universiti Teknologi PETRONAS  
Bandar Seri Iskandar  
32610 Tronoh  
Perak Darul Ridzuan**

# **CERTIFICATION OF APPROVAL**

## **Rag Layer Formation and Stability of Crude Oil Emulsion Under Different Imposed Mechanical Energy and Temperatures**

by

Rachael Tan Fern Fern

14858

A project dissertation submitted to the

Mechanical Engineering Programme

Universiti Teknologi PETRONAS

In partial fulfillment of the requirement for the

**BACHELOR OF ENGINEERING (Hons.)**

**(MECHANICAL)**

Approved by,

---

(AP Dr Azuraïen Binti Japper @ Jaafar)

UNIVERSITI TEKNOLOGI PETRONAS

TRONOH, PERAK

**January 2015**

## **CERTIFICATION OF ORIGINALITY**

This is to certify that I am responsible for the work submitted in this project, that the original work is my own except as specified in the references and acknowledgements, and that the original work contained herein have not been undertaken or done by unspecified sources or persons.

---

RACHAEL TAN FERN FERN

## ABSTRACT

Crude oil emulsion is a significant contributor of production losses in the Oil and Gas industry. The stability of the emulsion determines the magnitude of losses to be coped with by the industry. Several factors contribute to the stability of an emulsion hence this research was carried out to study the stability of crude oil emulsion and rag layer (unresolved emulsion) formation under four different imposed mechanical energy (by varying homogenizer speed) and two mixing temperatures using two types of crude oils. Five tests were conducted on each emulsion to study on the properties of the emulsions for a more comprehensive analysis. The five tests are bottle test (emulsion stability testing), Micro-Differential Scanning Calorimetry (Micro-DSC), Cross-Polarized Microscopy (CPM), rheological test (Rheometer) and titration test (water content determination). Crude Oil A produces water-in-oil emulsion while Crude Oil B produces oil-in-water emulsion. High mixing temperatures produce loose emulsions that do not have rag layer issues while the lower (mixing) temperature emulsions are tighter and forms rag layer. The imposed mechanical energy has a direct effect on the emulsion stability. The highest mixing speed produces the most stable emulsion while the lowest speed produces the least stable emulsion. The middle range mixing speeds on the other hand shows an inconsistency in its stability pattern. All the oil layers after separation meet the requirement set by the industry except for the highest mixing energy emulsion at 60°C. The regulations by the Environmental Quality Act 1974 for discharge water are also met by all water layers except for emulsion that was mixed with the highest mixing speed.

## **ACKNOWLEDGEMENT**

My heartfelt gratitude goes out to my supervisor, Associate Professor Dr Azuraïen Japper @ Jaafar, whose expertise, guidance and understanding contributed greatly to my Final Year Project experience.

Also, much appreciation goes to Petrus Tri Bhaskoro for the impartation of knowledge and hands on aid and guidance in the Flow Assurance Lab. Thanks also go out to the officers and technicians for the assistance provided at all levels of the research.

I would like to acknowledge Associate Professor Dr Hussain Hammud Ja'afar Al Kayiem for the contribution of his knowledge, time and feedbacks to this work. Special thanks also to my fellow colleagues, Matthew V George, Amirul Ariffin and Thevi Sreetharan for their technical assistance throughout the duration of this research. Thank you also to my seniors for their assistance in any matter possible.

A special thank you goes out also to my family for their unending support and encouragement throughout my undergraduate studies.

Last but not least, an acknowledgment to Universiti Teknologi PETRONAS for the great platform prepared for students to conduct research with high quality equipment and in a conducive and safe environment.

## TABLE OF CONTENTS

CERTIFICATION OF APPROVAL .....	i
CERTIFICATION OF ORIGINALITY .....	ii
ABSTRACT .....	iii
ACKNOWLEDGEMENT .....	iv
CHAPTER 1.....	1
1.1 Background of Study .....	1
1.2 Problem Statement .....	2
1.3 Objectives .....	3
1.4 Scope of Study .....	3
1.5 Relevancy and Feasibility of Study .....	4
CHAPTER 2.....	5
2.1 Formation of Crude Oil Emulsion .....	5
2.1.1 Classifications of Crude Oil Emulsion.....	5
2.1.2 Formation of Emulsion in Crude Oil Production.....	8
2.2 Crude Oil Properties that Affect Emulsion Formed .....	9
2.2.1 Surface-Active Agents .....	9
2.2.2 Viscosity and Density .....	10
2.3 Composition of Formation and Produced Water .....	11
2.4 Pressure and Temperature Profiles from Wellhead to Export Line.....	12
2.5 Production of Crude Oil Emulsion in Flow Assurance Lab .....	14
2.5.1 Duration of Emulsification and Water Cut .....	14
2.5.2 Flow Rate vs Homogenizer Speed .....	14
2.6 Rag Layer.....	16

2.6.1 Treatment Methods of Emulsion.....	17
2.6.2 Formation of Rag Layer .....	19
CHAPTER 3.....	20
3.1 Introduction.....	20
3.2 Flowchart .....	20
3.3 Experiment Methodology .....	21
3.3.1 Procedure.....	21
3.3.2 Materials and Apparatus.....	24
3.3.3 Data Analysis .....	25
3.4 Gantt Chart and Key Milestone .....	26
3.4.1 FYP 1 Timeline .....	26
3.4.2 FYP 2 Timeline .....	28
CHAPTER 4.....	29
4.1 Introduction.....	29
4.2 Rheological Properties .....	30
4.2.1 Wax Appearance Temperature.....	30
4.2.2 Viscosity.....	34
4.2.3 Yield Stress .....	37
4.3 Emulsion Stability.....	39
4.3.1 Crude A .....	39
a) Crude A at 60°C.....	45
b) Crude A at 80°C.....	48
4.3.2 Crude B .....	51
4.4 Water Content (Micro-DSC and Titrator).....	53
4.4.1 Emulsion.....	54

4.4.2 Rag Layer .....	54
4.4.3 Oil Layer .....	55
4.4.4 Water Layer.....	56
4.5 Droplet Size .....	57
4.6 Wax Crystals in Emulsion .....	58
CHAPTER 5.....	61
5.1 Conclusion and Future Works .....	61
REFERENCES.....	63
APPENDICES.....	66
Appendix I Calculation of Stirrer Speed of Crude A.....	66
Appendix II Calculation of Stirrer Speed of Crude B.....	68
Appendix III Rheometer results of Flow Temperature Ramp .....	70
Appendix IV Bottle test data of Crude A experiments .....	75

## LIST OF FIGURES

FIGURE 1.	Water-in-oil, Oil-in-water, Water-in-oil-in-water Emulsion Photomicrograph (Kokal, 2002) .....	6
FIGURE 2.	Temperature Profile of Pipeline in °C .....	13
FIGURE 3.	Pressure Profile of Pipeline in psia.....	13
FIGURE 4.	Simplified Representation of a Rag Layer (Morvarid, 2012).....	17
FIGURE 5.	Percent Loss by Volume vs Temperature (Smith and Arnold, 1987) ...	17
FIGURE 6.	Stirrer in Beaker for Emulsification .....	21
FIGURE 7.	Wax Appearance Temperature of Emulsion and Crude Oil A.....	33
FIGURE 8.	Flow Temperature Ramp Results from Rheological Test .....	34
FIGURE 9.	Viscosity at WAT against Mixing Speed for Emulsions formed at 60°C and Crude Oil A.....	35
FIGURE 10.	Amplitude Sweep Results from Rheological Test.....	37
FIGURE 11.	Yield Stress against Mixing Speed for Emulsions formed at 60°C and Crude Oil A.....	38
FIGURE 12.	Reduction of Volume of Emulsion of CRUDE A at 60°C and 80°C ....	39
FIGURE 13.	Total Volume of Oil Layer of CRUDE A at 60°C and 80°C.....	41
FIGURE 14.	Total Volume of Water Layer of CRUDE A at 60°C and 80°C .....	42
FIGURE 15.	Total Volume of Sample in Percentage of CRUDE A at 60°C and 80°C .....	43
FIGURE 16.	Rate of evaporation of Oil and Water at 60°C.....	44
FIGURE 17.	Rate of evaporation of Oil and Water at 80°C.....	44
FIGURE 18.	Volume of Layers in Percentage of Experiment A.....	45
FIGURE 19.	Volume of Layers in Percentage of Experiment B.....	45
FIGURE 20.	Volume of Layers in Percentage of Experiment C.....	46
FIGURE 21.	Volume of Layers in Percentage of Experiment D.....	47
FIGURE 22.	Rag Layer Volume in Percentage against Mixing Speed for Emulsions at 60°C .....	48
FIGURE 23.	Volume of Layers in Percentage of Experiment E.....	48
FIGURE 24.	Volume of Layers in Percentage of Experiment F .....	49
FIGURE 25.	Volume of Layers in Percentage of Experiment G.....	50

FIGURE 26.	Volume of Layers in Percentage of Experiment H.....	50
FIGURE 27.	Water Content in Emulsion .....	54
FIGURE 28.	Size of Water Droplet in Emulsion and Rag Layer at 60°C.....	57
FIGURE 29.	Microscopic Image of Wax Crystals for Emulsion A at 33°C and 60°C .....	58
FIGURE 30.	Microscopic Image of Wax Crystals for Emulsion B at 33°C and 55°C .....	58
FIGURE 31.	Microscopic Image of Wax Crystals for Emulsion C at 33°C and 60°C .....	59
FIGURE 32.	Microscopic Image of Wax Crystals for Emulsion D 33°C and 55°C ..	59

## LIST OF TABLES

TABLE 1.	Composition of Produced Water from Niger Delta (Opawale & Osisanya, 2013) .....	11
TABLE 2.	Composition of Produced Water from Henan Shuanghe Oilfield (Kang et al., 2011) .....	11
TABLE 3.	Composition of Formation Water from Berlian East-3 Well (Salleh, 2014) .....	12
TABLE 4.	Pipeline Properties of a Malaysian oil field .....	12
TABLE 5.	Flow Rate Sample Data for Malaysian Oil Fields .....	14
TABLE 6.	Selected Composition of Formation Water for Experiment .....	21
TABLE 7.	Stirrer Speed for Crude A at $T_a = 60^\circ\text{C}$ .....	23
TABLE 8.	Stirrer Speed for Crude A at $T_b = 80^\circ\text{C}$ .....	23
TABLE 9.	Stirrer Speed for Crude B at $T_a = 60^\circ\text{C}$ .....	23
TABLE 10.	Stirrer Speed for Crude B at $T_b = 80^\circ\text{C}$ .....	24
TABLE 11.	Rag Layer Volume Observation Time .....	25
TABLE 12.	Stirrer Speed used for the Formation of Emulsion in Laboratory .....	29
TABLE 13.	Parameters of Emulsions .....	29
TABLE 14.	WAT of Emulsions and CRUDE A at $60^\circ\text{C}$ from Rheometer and Micro-DSC .....	32
TABLE 15.	WAT of Emulsions and CRUDE A at $80^\circ\text{C}$ from Rheometer and Micro-DSC .....	32
TABLE 16.	Viscosity of Emulsions and CRUDE A at WAT .....	35
TABLE 17.	Model Equation for viscosity above WAT .....	36
TABLE 18.	Yield Stress of Emulsions and Crude Oil A .....	38
TABLE 19.	Likert Scale Data of Emulsions I, J, K and L .....	52
TABLE 20.	Likert Scale Data of Emulsions M, N, O and P .....	53
TABLE 21.	Oil and Water Composition of Rag Layer .....	55
TABLE 22.	Oil and Water Composition of Oil Layer .....	55
TABLE 23.	Oil and Water Composition of Water Layer .....	56

## **CHAPTER 1**

### **INTRODUCTION**

#### **1. INTRODUCTION**

##### **1.1 Background of Study**

The production of crude oil involves a highly complex process. As oil and gas reservoir matures, more water is produced along with crude oil. During transportation of crude oil through the production line, agitation energy is supplied from several sources such as chokes, pumps and wellheads (Kelesoglu, Pettersen and Sjoblom, 2012). These energies cause the crude oil, formation water, and solids to comingle with each other. This mixing motion results in the formation of crude oil emulsion.

Crude oil emulsion when allowed to settle will eventually separate into the oil and water phases. The stubborn emulsion that does not separate due to its tightness over time is known as rag layer. By definition rag layer is the undesirable mixture of water and oil dispersion along with the presence of solids (Saadatmand et al., 2008).

The formation of water-in-oil emulsion during the production of crude oil is highly unfavourable as the productivity and operations will suffer losses (Opawale and Osisanya, 2013). In order to eliminate the losses, oil and gas companies have come a long way in discovering the properties and behavior of emulsion and formation of rag layer for an effective management and solutions.

## 1.2 Problem Statement

Oil reservoirs naturally contain a mixture of fluids such as formation water, oil and gas and solid particles. During the extraction of crude oil from the reservoir, an event of a mixture of water and oil is inevitable. Along the flow from the reservoir to the export line, the oil and water mixture tend to turn into an emulsion due to the supply of agitation energy. Some of the sources of the mixing energy are the change in pressure through chokes, valves; turbulence due to the flow through well head and pipe as well as from pumps.

The formation of emulsion in the crude oil production is an undesirable occurrence as they cause financial and operational losses however it is unavoidable. The surrounding conditions and environment of crude oil extraction determines the stability of the emulsion formed. Formation of emulsion requires the existence of three main components which are two immiscible liquids, mixing energy and surfactant. Tight emulsions when left to settle, faces difficulty in separating into the oil and water phases. Additional expenses will be incurred to recover the oil from the tight emulsion formed. Therefore, the formation of emulsion is truly an undesirable state in oil production. To overcome the setback caused by emulsion formation, it is important for oil companies to identify conditions that cause the formation of either tight or loose emulsions as well as to find out the characteristics and properties of the emulsions formed. Additionally, an early understanding of the behaviour of emulsion formed is important for effective crude oil handling and for solutions readiness in overcoming emulsion problem.

### **1.3 Objectives**

The objectives of this project are:

- To replicate the formation of water-in-oil emulsion in the laboratory by mimicking the oil field environment
- To assess the formation and stability of emulsion and rag layer homogenized with variance in the mixing and settling temperatures and imposed mechanical energy
- To study and characterize the emulsion and rag layer formed

### **1.4 Scope of Study**

The research is carried out based on the pipeline data of a Malaysian oil field with water depth of 101m. This study involves two different types of crude oils which are identified as Crude A and Crude B. From the pipeline data, two temperatures between 30°C to 90°C were chosen for the experiments. A total of four different homogenizer speeds were identified to study on the effect of varying mechanical energy on the formation of crude oil emulsion. Overall there are sixteen experiments from the combination of all the manipulated variables.

The study includes observations of the oil and water particles under the cross-polarized microscope (CPM); obtaining data from the Micro-Differential Scanning Calorimeter (Micro-DSC); titration of emulsion for water content information; investigation of rheological properties of emulsion as well as bottle test to observe the stability of the emulsion based on the volume of rag layer formed over time.

The point of discussion with regards to the emulsion formed includes the thermodynamic stability of emulsion, the tightness of emulsion formed, size of water droplet in emulsion as well as the type of emulsion formed based ratio of the two immiscible liquid (e.g. water-in-oil, oil-in-water or water-in-oil-in-water).

## **1.5 Relevancy and Feasibility of Study**

Oil and gas companies are commonly faced with the issue of water-in-oil emulsion. The formation of emulsion affects the productivity of oil production by incurring additional expenses and causing unwanted losses to the company. With this study, the influence of different mechanical energy on the formation of emulsion and several other conditions such as temperature and type of crude oil is analysed and discussed. This will then serve as a reference to oil companies on the conditions to be avoided to prevent or minimize the formation of stable emulsions. Having said so, this study is proved to be relevant to the industry.

A total of sixteen experiments were carried out with each experiment requiring about one month of observations. Several experiments were carried out concurrently to save time. With a given duration of twenty eight weeks, the project works started in week 7 of semester 1 and ended in week 5 of semester 2 as shown in the Gantt chart in the subsequent chapters. This study is therefore feasible in time context. The materials used in this study were also readily available at the flow assurance laboratory in block 20 of Universiti Teknologi PETRONAS that allowed the experiments to take place smoothly.

## **CHAPTER 2**

### **LITERATURE REVIEW**

#### **2. LITERATURE REVIEW**

##### **2.1 Formation of Crude Oil Emulsion**

###### **2.1.1 Classifications of Crude Oil Emulsion**

Emulsion is typically formed with the mixing of two immiscible liquid (Leal-Calderon et al., 2007). The natural characteristics of immiscible liquids cause the mixture between two immiscible liquids to consist of dispersions of droplets of one liquid in another.

Over the years, several classifications of emulsion have been acknowledged. According to Opawale and Osisanya (2013), emulsions are divided into three types which are water-in-oil (W/O), oil-in-water (O/W) and multiple (water-in-oil-in-water, W/O/W). The W/O/W emulsion refers to emulsion with presence of water droplets in oil droplets in a continuous water phase. The type of emulsion is categorized according to the ratio of the two immiscible liquid present in an emulsion. The same classification has been observed and used by Kokal (2002) and Abdel-Raouf (2012).

Smith and Arnold (1987), states that an emulsion consists of two phases known as the dispersed or internal phase and the continuous or external phase. The phase of the liquid determines the type of emulsion. For example, a water-in-oil emulsion has water as the dispersed phase and oil as the continuous phase. Inversely, an oil-in-water emulsion has oil as the dispersed phase and water as the continuous phase. The basic rule in differentiating the phases of oil and water is by comparing the volume of both liquids. In line with Leal-Calderon et al. (2007), Kokal (2002) stated that the liquid with a much smaller volume compared to the other is identified as the dispersed phase while

the other liquid will be known as the continuous phase. Given a situation where the ratio of the liquids are almost the same (about 50:50), then other factors will be used to determine the type of emulsion.

The figure below shows the photomicrograph of a water-in-oil emulsion; an oil-in-water emulsion and a water-in-oil-in-water emulsion.

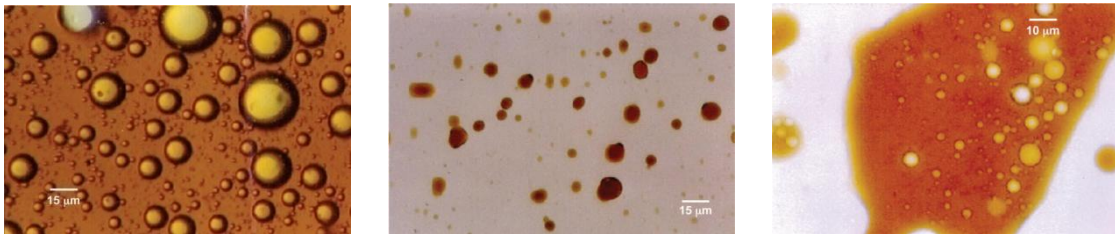


FIGURE 1. Water-in-oil, Oil-in-water, Water-in-oil-in-water Emulsion  
Photomicrograph (Kokal, 2002)

Slomkowski et al. (2011) has categorized emulsion based on the size of the particles of the dispersed phase. The three categories are macro-emulsion, mini-emulsion (also known as nano-emulsion) and micro-emulsion. Macro-emulsion has dispersed particle phase with diameters of about 1 to 100μm. This category of emulsion is “unstable” because it consists of large droplets that allow sedimentation to take place and separate between the dispersed and continuous phase. The rate of coalescence of the dispersed droplets of macro-emulsion is slow, caused by the presence of low-molecular-weight or polymeric surfactants.

The next category is known as the mini-emulsion or nano-emulsion. The size of the droplets ranges between 50nm to 1μm (Slomkowski et al., 2011). Mini-emulsion is stable against diffusion degradation by a compound insoluble in the continuous phase and hence is more stable than macro-emulsion. This emulsion is only stable kinetically. Rajalakshmi et al. (2011) suggested a droplet diameter range of 50-200nm while Jimtaisong (2007) suggested a range between 100 to 400nm.

Micro-emulsion on the other hand has droplets of diameters 1 to 100nm and is thermodynamically stable (Slomkowski et al., 2011 & Jimtaisong, 2007). The average diameter of the particles of the dispersed phase in an emulsion is about 1 millimeter ( $10^{-3}$ m). Since, micro- refers to  $10^{-6}$  and emulsion implies that droplets of the dispersed phase have diameters close to  $10^{-3}$ m, the micro-emulsion implies a system with the size range of the dispersed phase in the  $10^{-6} \times 10^{-3} = 10^{-9}$  m range (Slomkowski et al., 2011).

Pickering emulsions on the other hand have particles which reside at the interface and stabilize the emulsion. Particles which are more wetted by water than oil would stabilize oil-in-water emulsion and vice versa (Tadros, 2013).

Another three types of emulsion classifications are based upon the stability of the emulsion. In order to identify a stable emulsion, the emulsion must or usually have an increasing viscosity over time (Fingas and Fieldhouse, 2003). Contrarily, an unstable emulsion is identified when the separation between water and oil occurs in a speedy manner. Emulsions that are in between stable and unstable conditions are known as mesostable emulsions.

In agreement, Kokal (2002) has put this category in simpler words where he termed the categories as loose, medium and tight. Loose emulsion tend to separate within minutes; medium emulsion in tens of minutes and tight emulsion takes hours or days and the separation may occur only partially. The emulsion tightness index (ETI) formula by Opawale and Osisanya (2013) may be used to calculate the stability of the emulsion.

$$ETI = \left[ \frac{\text{Vol of water blended} - \text{Vol of water seperated after time, } t}{\text{Vol of water blended}} \right] \%$$

### **2.1.2 Formation of Emulsion in Crude Oil Production**

Smith and Arnold (1987) have agreed upon three vital criteria of emulsion formation which are:

1. Two different immiscible liquids must be present.
2. The presence of surfactants to stabilize dispersed phase droplets and/or
3. Adequate mixing energy is supplied to allow one liquid to disperse in the other liquid.

The three criteria mentioned above were stated again by Abdel-Raouf (2012).

Several surrounding conditions in crude oil production contribute to the formation of emulsion in the petroleum industry. The formation of emulsion may be the outcome of one or multiple sources of mixing energy. Along the production line of crude oil there are several areas where agitation occurs. Kelesoglu et al. (2012) and Smith and Arnold (1987), listed the instances where mixing energy is supplied during crude oil production and transportation:

1. pressure drop through chokes, valves, pipes and other surface equipment
2. flow through tubing, wellhead, manifold or flowlines
3. the surface transfer pump
4. bottom hole pump
5. wellbore

Operating practices that cause production of excess water due to poor cementing and flawed reservoir management, as well as process design that expose the oil-water mixture to excess turbulence amplifies emulsion problems. Preventable turbulence faced by oil-water mixture are normally due to over-pumping and poor maintenance of plunger and valves in rod-pumped wells, use of more gas lifts than needed and using pump where gravity flow could have been used (Smith and Arnold, 1987).

## **2.2 Crude Oil Properties that Affect Emulsion Formed**

The tendency of crude oil to emulsify depends on a number of factors. The biological tendency of a liquid-liquid system to separate and reduce its interfacial area that subsequently reduces the interfacial energy causes an emulsion to be labeled as thermodynamically unstable. A thermodynamically unstable emulsion can still be stable for a period of time due to kinetic stability (Kokal, 2002).

### **2.2.1 Surface-Active Agents**

Emulsion stability and behaviour relies greatly on the presence of adsorbed structures on the interface between the two liquid phases (Abdel-Raouf, 2012). The natural properties of oil are a complex matter that impacts the formation of crude oil emulsion. Rodionova et al. (2014), Tadros (2013) and Abdel-Rouf (2012) have agreed upon the idea of the presence of surface-active agents or surfactants as the stabilizing agent of an emulsion that becomes concentrated at the oil-water interface where interfacial films are formed. The molecules of surfactants have the ability to interact and/or reorganize at the oil-water interface. This phenomenon reduces the interfacial tension which in response encourages dispersion and emulsification of water droplets in crude oil (Smith and Arnold, 1987).

One example of natural surfactant is asphaltenes, which is a high molecular weight polar component. Wax crystals, resins, porphyrins and fatty acids (naphthenic acid) are some active surface agents that aid asphaltenes in stabilizing the emulsion formed. Resins solubilize asphaltenes while waxes co-adsorb at the interface. Fatty acids on the other hand support the formation of emulsion by creating an ideal environment through the balancing of pH levels (Abdel-Raouf, 2012). On top of that, Tadros (2013) also mentioned that the presence of surfactants will reduce the interfacial tension which allows the droplet to be broken down more easily.

Besides surfactants, species that adsorb at the oil-water interface and prevent drop growth and phase separation into the original oil and water phases; can stabilize an emulsion. After adsorption, the surfaces will turn visco-elastic and provide stability to the emulsion (Abdel-Raouf, 2012).

### 2.2.2 Viscosity and Density

A higher density crude oil (low API gravity) forms a larger volume and more stable emulsion than a lower density crude oil (Smith and Arnold, 1987). Concomitantly, crude oil with higher viscosity tends to form emulsion with higher stability when weighed against low viscosity crude oil. The viscous property of crude oil causes the formation of a stable emulsion as the movement of the dispersed water droplets in the emulsion is retarded; as a result the coalescence is impeded. Paraffin-based oils have a lower emulsification tendency than asphaltic-based oils. Also, high density and high-viscosity oils have a larger volume of emulsifiers in comparison to lighter oils (Smith and Arnold, 1987).

Pure crude oil in an emulsion is normally less viscous than the emulsion itself. According to Smith and Arnold (1987), the ratio of the viscosity of emulsion to the viscosity of pure crude oil in an oilfield depends on the shear rate supplied. For many emulsions and for shear rates normally encountered in piping systems, the ratio can be estimated using the equation below.

$$\frac{\mu_e}{\mu_o} = 1 + 2.5f + 14.1f^2$$

Where,  $\mu_e$ =viscosity of emulsion  
 $\mu_o$ =viscosity of pure crude oil  
 $f$ =fraction of the dispersed phase

### 2.3 Composition of Formation and Produced Water

Oil and gas reservoirs are naturally made up of gas, oil and water along with the presence of solid particles. As the oils are being extracted from the reservoir, water is extracted alongside. The naturally occurring water is known as formation water (Ekens et al., 2005). Produced water on the other hand refers to water produced during oil and gas production. It is the mixture of naturally occurring formation water, the re-injected water and chemical injected during production. Alternatively, produced water is also a result of oil and gas production from below the sea reservoirs where the water contains a certain amount of hydrocarbons as well (International Association of Oil and Gas Producers, 2002).

Opawale and Osisanya (2013) gave an example of a composition of produced water from Nigeria in the Niger Delta region as shown in the Table 1.

TABLE 1. Composition of Produced Water from Niger Delta (Opawale & Osisanya, 2013)

Composition	$K^+Na^+$	$Mg^{2+}$	$Ca^{2+}$	$Cl^-$	$SO_4^{2-}$	$HCO_3^-$	$CO_3^{2-}$
Mass (mg/L)	1452.2	5.6	16.8	425.5	20.2	2927.7	121.1

Table 2 gives the composition of the Shuanghe waste water from the oil-water treatment center of Henan Shuanghe oilfield reported by Kang et al. (2011). The total salinity in the water is about 5251 mg/L and oil concentration is roughly of 417 mg/L. The water is alkaline with a pH of 8.6.

TABLE 2. Composition of Produced Water from Henan Shuanghe Oilfield (Kang et al., 2011)

Salt	$K^+Na^+$	$Mg^{2+}$	$Ca^{2+}$	$Cl^-$	$SO_4^{2-}$	$HCO_3^-$	Sulphide
Mass (mg/L)	1689.8	66.8	17.7	1496.4	58.6	1921.7	30-40

Table 3 provides the information of formation water in Berlian East-3 (M213 reservoir) where the location of the reservoir is about 25km offshore peninsular Malaysia. The formation water has a pH value of 8.14 at 22°C. This analysis was obtained from Berlian Field Database (Salleh, 2014).

TABLE 3. Composition of Formation Water from Berlian East-3 Well  
(Salleh, 2014)

Ions	Na <sup>+</sup>	Mg <sup>2+</sup>	Ca <sup>2+</sup>	Ba <sup>2+</sup>	Iron	Cl <sup>-</sup>	SO <sub>4</sub> <sup>2-</sup>	HCO <sub>3</sub> <sup>-</sup>	CO <sub>3</sub> <sup>2-</sup>
Mass (mg/L)	10600	18.8	26.4	18.9	<2	12212	89	7115	54

#### 2.4 Pressure and Temperature Profiles from Wellhead to Export Line

During the flow of crude oil in the pipeline, the temperature varies significantly with little variation in the pipeline pressure. The data below is collected from a Malaysian oil field with a water depth of 101m. The pipeline length is 12.9km and with four risers present, the total distance is 13.6km. Table 4 below shows the pipeline properties, while the subsequent figures show the temperature and pressure profiles of the pipeline.

TABLE 4. Pipeline Properties of a Malaysian oil field

Parameters	Unit	Pipeline from WHP-A to WHP-B
Nominal Diameter	inch	26
Pipeline Length	km	12.9
Pipeline Length (including risers)	km	13.6
Pipe Inner Diameter (Zone 1/Zone 2)	inch	24

Figure 2 and Figure 3 shows the temperature and pressure profile of the pipeline in a Malaysian oil field.

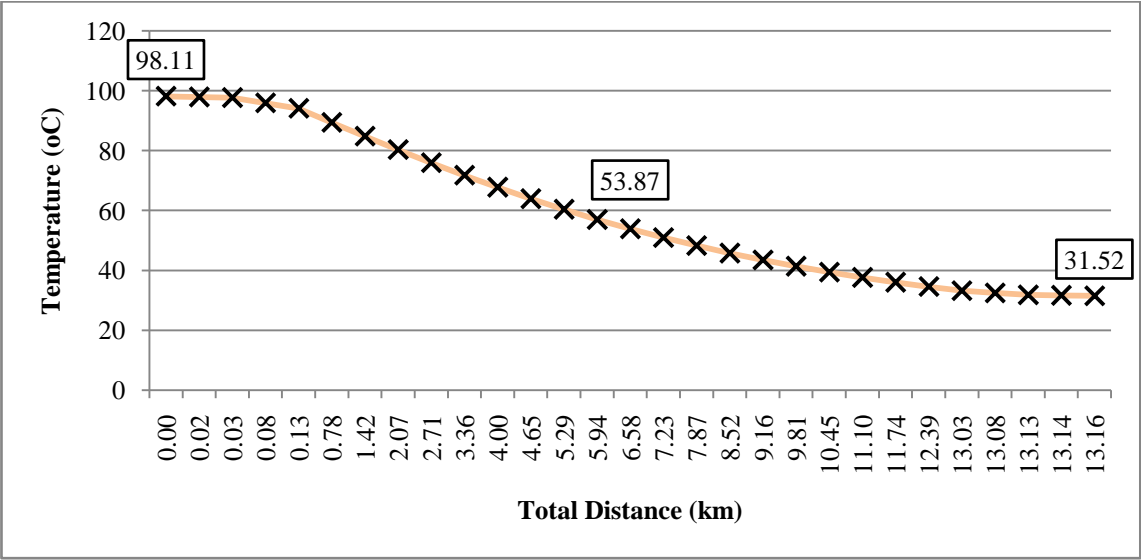


FIGURE 2. Temperature Profile of Pipeline in °C

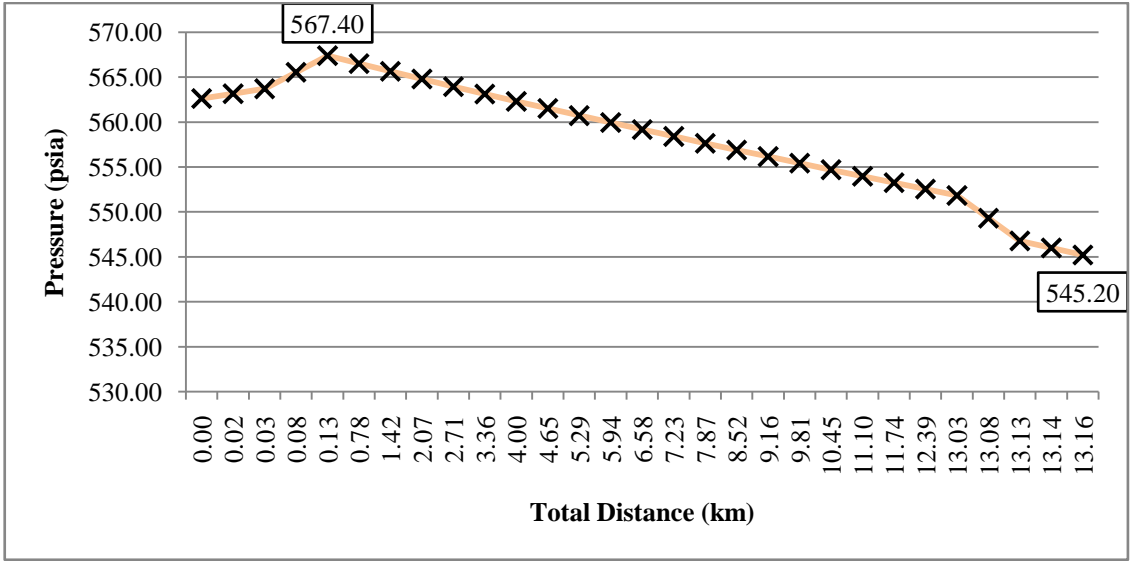


FIGURE 3. Pressure Profile of Pipeline in psia

## 2.5 Production of Crude Oil Emulsion in Flow Assurance Lab

### 2.5.1 Duration of Emulsification and Water Cut

Kokal and Al-Juraid (1999) used an automatic shaker to mix the oil and water mixture for approximately five minutes whereas Rodionova et al. (2014) allowed the oil-water mixture to be agitated for fifteen minutes. Along the same line, Kang et al. (2011), allowed the water and oil mixture to be agitated for ten minutes.

Also, through Kokal and Al-Juraid's (1999) study, they found that the average water cut of emulsions in a large Saudi Arabian field which produces from seven different reservoirs is 26.8%. The range of water cut obtained in another study is between 5 to 52% (Opawale and Osisanya, 2013). Hence, an average water cut of 30% is assumed in this study.

### 2.5.2 Flow Rate vs Homogenizer Speed

To obtain a reliable result on the formation and stability of rag layer, the conditions and environment where the emulsion is formed must reflect the pipeline conditions in the field. Below are several flow rate data obtained for oil fields in Malaysia.

TABLE 5. Flow Rate Sample Data for Malaysian Oil Fields

Field	Flow Rate (BBL/Day)
1	4110
2	3512
3	2824
4	2303
5	1622

According to Fingas and Fieldhouse (2003), the flow rate of emulsion in the pipeline can be mimicked by supplying equivalent kinetic energy through the stirrer.

$$\text{Kinetic Energy, } KE = \frac{1}{2}MV^2$$

Where,  $M = \text{mass (kg)}$   
 $V = \text{velocity } (\frac{m}{s})$

Supporting the equation above, Opawale and Osisanya (2013) proposed that the kinetic energy of a rotational device is:

$$KE = \frac{1}{2} M_s \left( \frac{2\pi N}{60} \times R_a \right)^2$$

Where,  $M_s = \text{mass of top bottle arm system} + \text{mass of total sample (kg)}$   
 $N = \text{Number of revolutions per minute (RPM)}$   
 $R_a = \text{Radius of arm (m)}$

As observed, the work in the pipeline is assumed to be equal to the amount of kinetic energy produced by rotational device (Fingas and Fieldhouse, 2013). Hence, the measure of work in the pipeline can be calculated below.

Consistent with Newton's second law,

$$F = ma = \dot{m}v$$

Where,  $F = \text{force (N)}$   
 $m = \text{mass (kg)}$   
 $\dot{m} = \text{mass flow rate } (\frac{kg}{s})$   
 $v = \text{velocity } (\frac{m}{s})$

$$Work = F \times D$$

Where,  $F = \text{force (N)}$   
 $D = \text{length of pipe (m)}$

The stirrer in the lab usually has a much smaller energy supply capacity as compared to the energy encountered in the oil fields. Therefore, Opawale and Osisanya (2013) suggested that the mixing speed is scaled down.

## 2.6 Rag Layer

Emulsion may cause formation of undesirable rag layer. Typically, rag layer is a mixture of flocculated water and oil droplets, fine solids and emulsified oil and water, as well as multiple emulsions (Khatri, 2010). Rag layer is observed as a viscous layer normally forming between the oil and water phase containing oil, water and solid, post settling (Czarnecki et al., 2007).

Varadaraj and Brons (2007) described rag layer as a micro-heterogeneous complex fluid of oil-in-water-in-oil dispersions throughout a continuous oil phase while Saadatmand et al. (2008) suggested that the rag layer is a loose structure of layered materials at the interface instead of a consolidated matrix of solids and emulsions. Rag layer most commonly occur in heavy crude oils with American Petroleum Institute (API) gravity of below 20.

Generally, rag layer is defined as a layer that prevents complete separation of two fluid phases and hence lowers the overall recovery of oil (Morvarid, 2012). Rag layer mainly consist oil, water and solids. Conclusively, the authors refer to rag layer as a complex multiple emulsion.

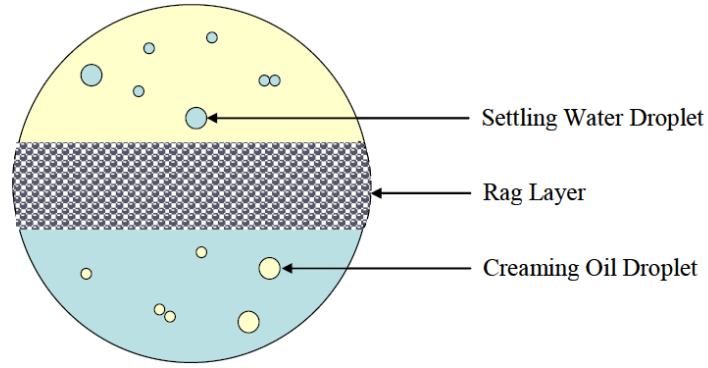


FIGURE 4. Simplified Representation of a Rag Layer (Morvarid, 2012)

### 2.6.1 Treatment Methods of Emulsion

Heating is one of the simplest methods to treat crude oil emulsion. Firstly, according to Smith and Arnold (1987) and Khatri (2010), the supply of heat will increase the molecular movements of the droplets of the dispersed phase causing greater collision forces between water droplets that will allow the droplets to settle more quickly. The difference in density between oil and water is also increased through heating thus accelerating the sedimentation and creaming rate.

Heating well fluid is however, expensive. The addition of heat to well fluids may cause significant losses of the lower-boiling-point hydrocarbons which will result in the loss of volume of the oil (Smith and Arnold, 1987). The figure below illustrates the volume losses vs temperature for 33°API crude.

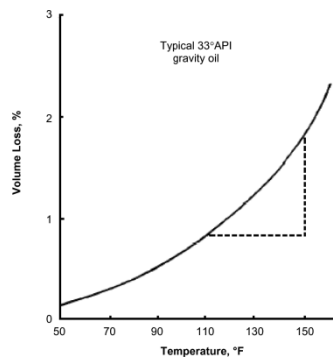


FIGURE 5. Percent Loss by Volume vs Temperature (Smith and Arnold, 1987)

Demulsifiers can be dissolved into the emulsion and the effect of treating chemicals may be enhanced with heat. Consequently, the chemicals work more effectively in breaking the film surrounding the droplets of the dispersed phase of the emulsion as the thermal energy provided also weakens and ruptures the interfacial film between oil and water leading to increased coalescence (Smith and Arnold, 1987 & Khatri, 2010).

Gravity settling is another method used to treat emulsion and is one of the most favoured due to its simplicity (Smith and Arnold, 1987). The difference in density of the oil and water causes the water to settle through and out of the oil. Since, water droplets are heavier than the oil phase; the droplets naturally have a downward gravitational force. This causes the droplets to settle at the bottom of the vessel.

From Stokes' law,

$$v = \frac{1.78 \times 10^{-6} (\Delta\gamma_{ow}) d^2}{\mu_o}$$

Where,  $v$ =downward velocity of the water droplet relative to the oil (ft/sec)  
 $d$ =diameter of the water droplet ( $\mu\text{m}$ )  
 $\Delta\gamma_{ow}$  =difference in specific gravity between the oil and water  
 $\mu_o$ =dynamic viscosity of the oil

From the equation above, it can be deduced that, the larger the size of water droplet and the larger the difference in density of the water and oil droplets, the higher is its downward velocity and the faster it settles (Smith and Arnold, 1987). This method is also commonly used in the laboratory to separate emulsion to form rag layer (Morvarid, 2012).

Emulsion droplets will go through sedimentation and creaming before separating into its individual phases. Before the sedimentation and creaming process, droplets will accumulate at the water-oil interface until coalescence occurs due to the intermediate density (Khatri, 2010).

### **2.6.2 Formation of Rag Layer**

There are a few mechanisms on rag layer formation. Saadatmand et al. (2008) and Morvarid (2012) used two mechanisms to explain the formation of rag layer. The first mechanism is a mechanical barrier and the second one is slow coalescence. An accumulation of oil-wet materials may occur at the planar interface of oil and water. This creates a barrier that prevents water and solid particles from passing through and hence impedes coalescence from taking place and encourages the formation of rag layer. The rag layer accumulation and build-up of interfacial material hinders droplet coalescence by trapping droplets in the stable network. The droplets are not able to settle through the interface until coalescence to larger droplets takes place. Through this, a rag layer can accumulate.

A third mechanism was suggested by Morvarid (2012) as the intermediate density. The rag layer density which is composed of water, oil and solids favours stability between the two fluid phases. Multiple emulsions of oil-in-water-in-oil produce droplets with an apparent density in between the water and organic phase densities. Therefore, due to the low inertial contribution of water droplets and the build-up of interfacial material, water droplets are prevented from coalescing, subsequently causing rag layer to be formed.

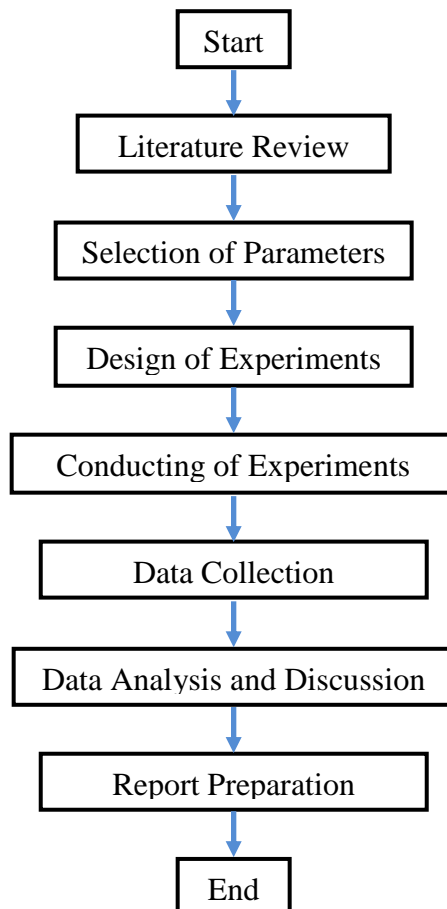
## CHAPTER 3 METHODOLOGY

### 3. METHODOLOGY

#### 3.1 Introduction

This chapter presents the flowchart, Gantt chart, experiment parameters and experiment methodology. The purpose of this research is to study the rag layer formation and stability of crude oil emulsion under different imposed mechanical energy and temperatures.

#### 3.2 Flowchart



### 3.3 Experiment Methodology

#### 3.3.1 Procedure

##### 1. Preparation of formation water.

Parameters:

- Homogenizer speed: 400RPM
- Duration of stirring: 1 hour
- Type of water used: Ultra pure water

TABLE 6. Selected Composition of Formation Water for Experiment

Substance	Concentration (g/L)
NaHCO <sub>3</sub>	5.1260
KCl	0.2646
NaCl	6.0114
BaCl:2H <sub>2</sub> O	0.0067
SrCl <sub>2</sub> :6H <sub>2</sub> O	0.0141
MgCl:6H <sub>2</sub> O	0.0750
CaCl:2H <sub>2</sub> O	0.2344

##### 2. Formation of emulsion.

The oil-water mixture is homogenized at varying speeds and temperatures using a homogenizer in a 100mL beaker.



FIGURE 6. Stirrer in Beaker for Emulsification

Parameters:

- Water cut is set at 30:70 and kept constant
- Volume of emulsion: 100mL
- Duration of emulsification: 15 minutes
- Mixing temperatures:  $T_a$  is 60°C and  $T_b$  is 80°C.
- Homogenizer speed: 3200, 5200, 7200, 9200 RPM

As recommended by Opawale and Osisanya (2013) to scale down the mixing speed, a ratio of 1:4 is used to obtain the homogenizer speed utilized in the laboratory. This scale was chosen due to the limited speed range of the IKA T25 stirrer that is between 3000 to 25000RPM as well as to avoid splashing during mixing due to the small sample volume. The speed of homogenizer used to conduct the experiment was selected from the data shown in Table 7, 8, 9 and 10. The detailed data of the calculation using Microsoft Excel is shown in Appendix I and Appendix II for two crude oils at  $T_a = 60^\circ\text{C}$  and  $T_b = 80^\circ\text{C}$ .

The equation to calculate the stirrer speed (RPM) from flow rate (bbl/day) is shown below.

$$\text{Kinetic Energy, } KE = \frac{1}{2}MV^2$$

Where,  $M = \text{mass (kg)}$

$V = \text{velocity } (\frac{m}{s})$

Supporting the equation above, Opawale and Osisanya (2013) proposed that the kinetic energy of a rotational device is:

$$KE = \frac{1}{2} M_s \left( \frac{2\pi N}{60} \times R_a \right)^2$$

Where,  $M_s = \text{mass of top bottle arm system} + \text{mass of total sample (kg)}$

$N = \text{Number of revolutions per minute (RPM)}$

$R_a = \text{Radius of arm (m)}$

Consistent with Newton's second law,

$$F = ma = \dot{m}v$$

Where,

$$F = \text{force (N)}$$

$$m = \text{mass (kg)}$$

$$\dot{m} = \text{mass flow rate } \left(\frac{\text{kg}}{\text{s}}\right)$$

$$v = \text{velocity } \left(\frac{\text{m}}{\text{s}}\right)$$

$$\text{Work} = F \times D$$

Where,

$$F = \text{force (N)}$$

$$D = \text{length of pipe (m)}$$

TABLE 7. Stirrer Speed for Crude A at  $T_a = 60^\circ\text{C}$

Field	Flow Rate, Q (bbl/day)	Flow Rate, Q ( $\text{m}^3/\text{s}$ )	Stirrer Speed (RPM)
1	2824	0.005196908	9006
2	2303	0.004238130	7344
3	1622	0.002984910	5172
4	978	0.001799779	3118

TABLE 8. Stirrer Speed for Crude A at  $T_b = 80^\circ\text{C}$

Field	Flow Rate, Q (bbl/day)	Flow Rate, Q ( $\text{m}^3/\text{s}$ )	Stirrer Speed (RPM)
1	2824	0.005196908	9064
2	2303	0.004238130	7392
3	1622	0.002984910	5206
4	978	0.001799779	3091

TABLE 9. Stirrer Speed for Crude B at  $T_a = 60^\circ\text{C}$

Field	Flow Rate, Q (bbl/day)	Flow Rate, Q ( $\text{m}^3/\text{s}$ )	Stirrer Speed (RPM)
1	2824	0.005196908	9074
2	2303	0.004238130	7400
3	1622	0.002984910	5212
4	978	0.001799779	3142

TABLE 10. Stirrer Speed for Crude B at  $T_b = 80^\circ\text{C}$

Field	Flow Rate, Q (bbl/day)	Flow Rate, Q ( $\text{m}^3/\text{s}$ )	Stirrer Speed (RPM)
1	2824	0.005196908	8998
2	2303	0.004238130	7338
3	1622	0.002984910	5168
4	978	0.001799779	3116

3. Once the emulsion is formed, the sample was separated into two test bottles.
  
4. The first bottle B1 was meant for rheological assessment, water content measurement, cross polarized microscopy (CPM) and thermodynamic event assessment over certain temperature ranges of the emulsion using a Micro-Differential Scanning Calorimeter (Micro-DSC).
  
5. The other test bottle (B2) was left for bottle test observations and the rag layer volume assessment for a period of one month.

### 3.3.2 Materials and Apparatus

The samples used were two types of crude oils which are identified as Crude A and Crude B. The important properties of the crude oils such as WAT and viscosity are recorded and shown in Chapter 4 along with the respective results. The composition of the formation water is mentioned in section 3.3.1. Among the materials needed for the formation water are  $\text{NaHCO}_3$ ,  $\text{KCl}$ ,  $\text{NaCl}$ ,  $\text{BaCl}\cdot 2\text{H}_2\text{O}$ ,  $\text{SrCl}_2\cdot 6\text{H}_2\text{O}$ ,  $\text{MgCl}\cdot 6\text{H}_2\text{O}$  and  $\text{CaCl}\cdot 2\text{H}_2\text{O}$ . Ultra pure water was utilized in the production of artificial formation water because of the high purity level from all contaminant including organic and inorganic compounds, dissolved and particulate matter as well as gases.

A 100mL Pyrex beaker was used for the mixing process of water-in-oil emulsion. A high speed stirrer (IKA T25 DS2) was placed into the beaker to supply the mixing energy to the water-oil mixture to agitate the mixture. Besides, an oil bath was also used

to heat the oil-water mixture to the desired temperature. Once ready, the emulsion was poured into two separate test bottles. On top of that, a timer and a thermometer were used to keep track of the time and to ensure that the temperature is at the desired value.

### 3.3.3 Data Analysis

For a thorough and reliable study, five analyses are conducted on each of the experiments. First, the cross-polarized microscope (CPM) test was conducted to capture the microscopic image of the rag layer and emulsion for size of water droplet and wax crystals analysis. Second observation is on the thermal activity using a Micro-Differential Scanning Calorimeter (Micro-DSC). The titration method was used to assess the water content in the crude oil emulsion. A rheometer was used to measure the viscosity and other rheological parameters of the emulsion. Finally, the volume of rag layer formed was recorded based on the time frame listed in the table below.

TABLE 11. Rag Layer Volume Observation Time

5 <sup>th</sup> minute	15 <sup>th</sup> minute	30 <sup>th</sup> minute	1 <sup>st</sup> hour	2 <sup>nd</sup> hour	4 <sup>th</sup> hour	Day 1	Day 2
Day 3	Day 4	Day 5	Day 6	Day 7	Week 2	Week 3	Week 4

### 3.4 Gantt Chart and Key Milestone

#### 3.4.1 FYP 1 Timeline

No	Activity	Week													
		1	2	3	4	5	6	7	8	9	10	11	12	13	14
1.0	Selection of project topic	█	█												
2.0	Preliminary research work		█	█	█	█									
2.1	Literature review		█	█	█	█									
2.1.1	Emulsion Formation			█	█										
2.1.2	Crude oil properties towards emulsion			█	█										
2.1.3	Composition of produced water				█	█									
2.1.4	Pressure and temperature profiles from well head to export line				█	█									
2.1.5	How to replicate crude oil emulsion mixing in lab				█	█									
3.0	Submission of extended proposal					█	★								
4.0	Design of experiment					█	█								
4.1	Identifying apparatus					█	█								
4.2	Sketching of experiments					█	█								
4.3	Identifying standards for experiments					█	█								
5.0	Proposal defense								█	█					

No	Activity	Week														
		1	2	3	4	5	6	7	8	9	10	11	12	13	14	
6.0	Project work															
6.1	4 out of 16 experiments															
6.2	8 out of 16 experiments															
6.3	Data compilation															
7.0	Submission of interim draft report														★	
8.0	Submission of interim report															★

### 3.4.2 FYP 2 Timeline

No	Activity	Week														
		1	2	3	4	5	6	7	8	9	10	11	12	13	14	15
1.0	Project work															
1.1	12 out of 16 experiments															
1.2	16 out of 16 experiments															
1.3	Data compilation															
2.0	Submission of progress report							★								
3.0	Data analysis and discussion															
3.1	Tabulation of data															
3.2	Review of data (discussion)															
4.0	Pre-SEDEX										★					
5.0	Submission of draft of final report											★				
6.0	Submission of dissertation (soft bound)												★			
7.0	Submission of technical paper												★			
8.0	Viva													★		
9.0	Submission of project dissertation (hard bound)															★

**CHAPTER 4**  
**RESULTS AND DISCUSSION**

**4. RESULTS AND DISCUSSION**

**4.1 Introduction**

Experiments started with the formation of emulsion using Crude A and Crude B at 60°C. The stirrer speeds used in the laboratory for the formation of emulsion are listed in Table 12. The stirrer speed was calculated and selected based on the flow rate in the field as mentioned in previous chapter. In this chapter, the emulsion is labeled (A, B, C, etc.) and the detail of each emulsion is as in Table 13.

TABLE 12. Stirrer Speed used for the Formation of Emulsion in Laboratory

	<b>Stirrer Speed (RPM)</b>
1	9200
2	7200
3	5200
4	3200

TABLE 13. Parameters of Emulsions

<b>Name</b>	<b>Crude Oil</b>	<b>Temperature</b>	<b>Stirrer Speed (RPM)</b>
A	CRUDE A	60°C	9200
B	CRUDE A	60°C	7200
C	CRUDE A	60°C	5200
D	CRUDE A	60°C	3200
E	CRUDE A	80°C	9200
F	CRUDE A	80°C	7200
G	CRUDE A	80°C	5200
H	CRUDE A	80°C	3200

I	CRUDE B	60°C	9200
J	CRUDE B	60°C	7200
K	CRUDE B	60°C	5200
L	CRUDE B	60°C	3200
M	CRUDE B	80°C	9200
N	CRUDE B	80°C	7200
O	CRUDE B	80°C	5200
P	CRUDE B	80°C	3200

## 4.2 Rheological Properties

### 4.2.1 Wax Appearance Temperature

Once emulsion is formed, the wax appearance temperature of emulsion is measured using the Micro-Differential Scanning Calorimeter (Micro-DSC) and the Rheometer. Using the Micro-DSC, the wax appearance temperature (WAT) can be obtained by studying the exothermic reaction of the crystallization process. As the emulsion sample is cooled from the maximum temperature, the emulsion starts to release heat as crystals are being formed and this temperature is identified as the wax appearance temperature. The Onset temperature obtained from the Micro-DSC data is recorded as the WAT.

Alternatively, the WAT can be determined from results obtained from the rheometer when the sample is put through a flow temperature ramp (constant shear rate) and oscillatory temperature ramp (constant frequency). During flow temperature ramp, the point where the viscosity starts to rise with decrease in temperature is determined as the WAT. Similarly, during oscillatory temperature ramp the point where loss modulus ( $G''$ ) or storage modulus ( $G'$ ) starts to increase with decreasing temperature is determined as the WAT. For the flow temperature ramp, the shear rate is constant at 10 1/s. The angular frequency of the oscillatory temperature ramp is kept constant at 10 rad/s.

Nevertheless, the WAT results produced by Micro-DSC has higher accuracy due to the ability of the equipment in capturing the slightest exothermic activity as compared to the rheometer which may require a minimum amount of crystallization before being able to capture the effect on viscosity,  $G'$  and  $G''$ .

The Micro-DSC and rheometer test were conducted for emulsions of Crude A that was mixed with varying homogenizer speeds at a temperature of 60°C. Since emulsion formed with Crude at 80°C and Crude B at both 60°C and 80°C are loose and can separate immediately, rheometer test was not conducted. The WAT of emulsions of Crude A at 80°C can still be obtained using the Micro-DSC.

The WAT is an important property of an emulsion as the calibration of equipments used during production, storage and transportation relies on this information for smooth operations. Setup of equipments below the wax appearance temperature of either the emulsion or crude oil may cause disruption to the extraction process. A temperature below the wax appearance temperature will cause the material to solidify causing problems in the transport of oil from the reservoir to the refinery or other final destinations.

Table 14 shows the WAT obtained from both Micro-DSC and rheometer for Crude Oil A and emulsions of Crude A at 60°C. For Emulsions A, B, C, and D, as the mixing speed decrease, the trend of WAT of the emulsions is observed to decrease. The Micro-DSC data observes a slightly higher WAT by Emulsion D as compared to Emulsion C. When comparing WAT of the Crude Oil A to the emulsions, all emulsions at 60°C recorded higher WAT than the crude oil itself.

TABLE 14. WAT of Emulsions and CRUDE A at 60°C from Rheometer and Micro-DSC

Sample	Wax Appearance Temperature (°C)			
	Rheometer		Micro-DSC	
	Flow	Oscillatory	Run 1	Run 2
A	42.847	42.697	41.342	40.938
B	42.532	42.580	41.169	41.498
C	41.879	42.444	40.436	41.202
D	41.847	41.809	40.468	40.823
CRUDE OIL A	41.665	39.384	≈39	≈39

The WAT obtained from Micro-DSC for emulsions formed at 80°C is shown in Table 15. At 80°C, as the mixing speed decrease, the WAT of the emulsions is observed to increase except for Emulsion C where there is a sudden drop from the trend. This pattern is different than that observed for emulsions at 60°C. When compared to the WAT of the crude oil, similar to what was observed before, all the emulsions at 80°C recorded higher WAT than pure Crude Oil A.

TABLE 15. WAT of Emulsions and CRUDE A at 80°C from Rheometer and Micro-DSC

Sample	Wax Appearance Temperature (°C)			
	Rheometer		Micro-DSC	
	Flow	Oscillatory	Run 1	Run 2
E	N/A	N/A	41.103	41.259
F	N/A	N/A	41.136	41.119
G	N/A	N/A	40.873	40.921
H	N/A	N/A	41.169	41.251
CRUDE OIL A	41.665	39.384	≈39	≈39

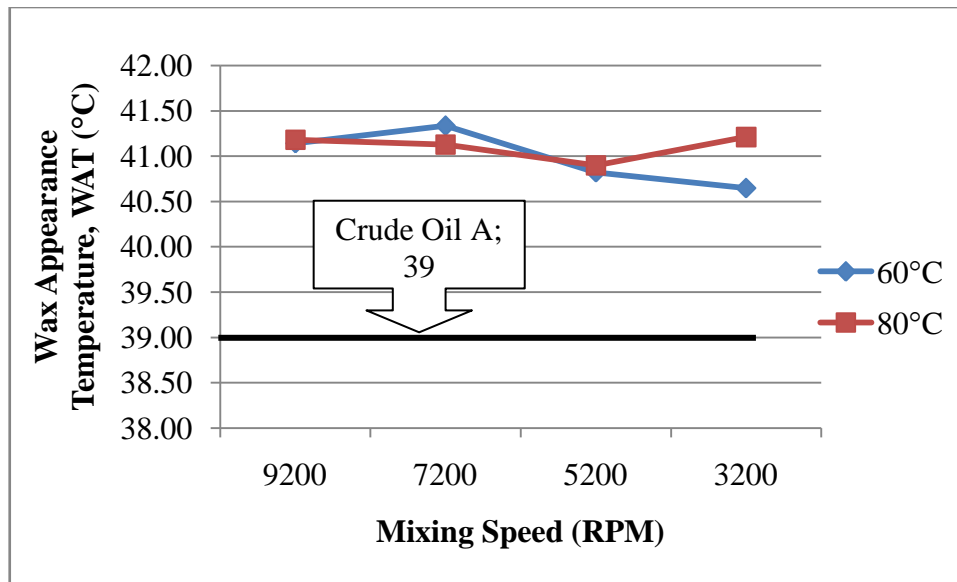


FIGURE 7. Wax Appearance Temperature of Emulsion and Crude Oil A

Figure 7 shows the relationship between the WAT (mean of two Micro-DSC runs), mixing temperature and mixing speed. At 60°C, the WAT is observed to decrease with decreasing mixing speed while at 80°C the trend of WAT is slightly increasing with decreasing speed. The fluctuation of the WAT is only within a  $\pm 1^\circ\text{C}$  range. The WAT of emulsions is observed to be higher than the WAT of the pure crude oil.

## 4.2.2 Viscosity

### a) Flow Temperature Ramp

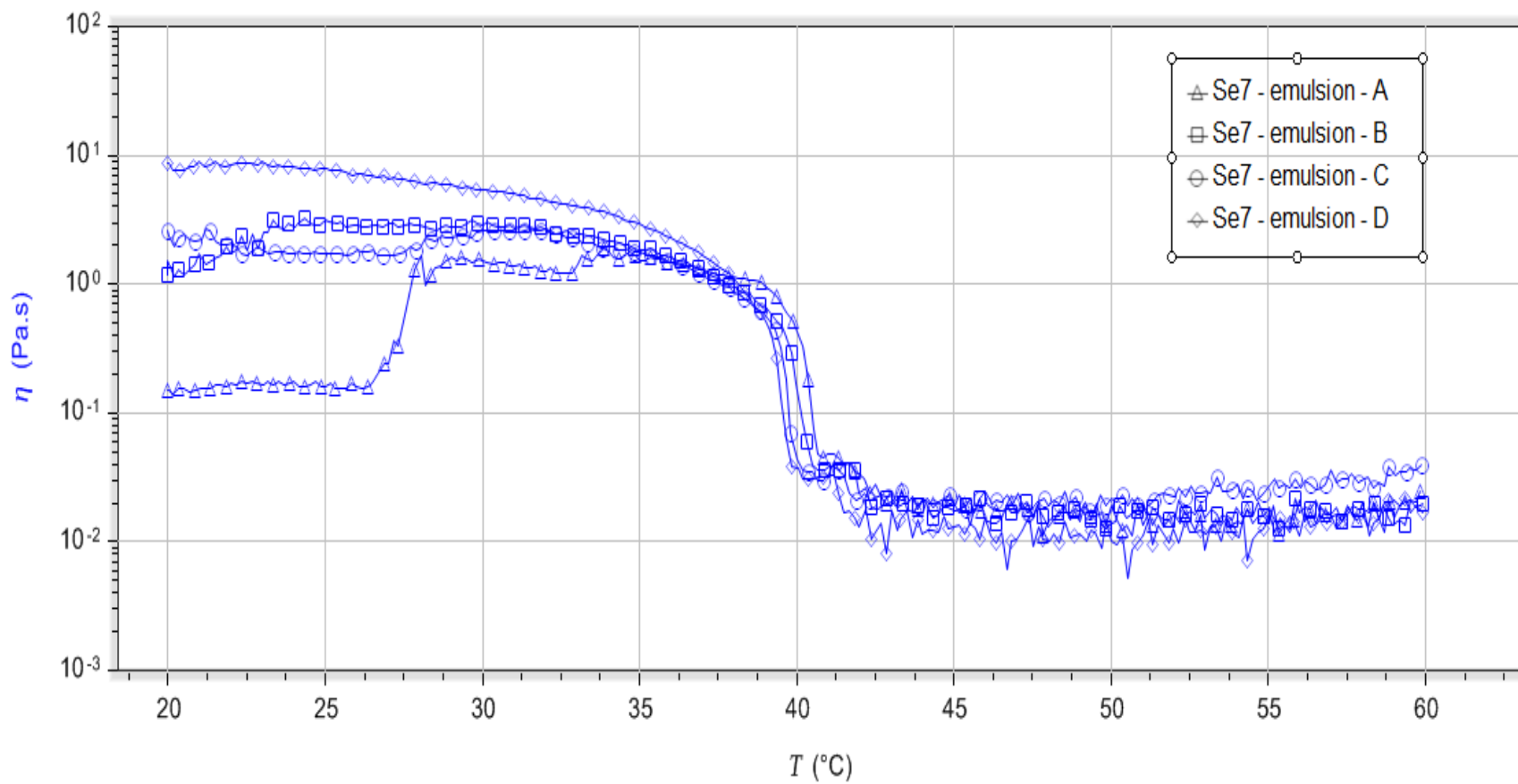


FIGURE 8. Flow Temperature Ramp Results from Rheological Test

i) Viscosity at WAT

The viscous property of crude oil and its emulsions is a vital a factor that determines the ease of transportation of crude oil. From the data, as the mixing speed increase, the viscosity of emulsion is higher. This supports the hypothesis that a higher speed produces smaller water droplets that causes viscosity to increase. Emulsions A and C have higher viscosity than Crude Oil A while Emulsion B and D have lower viscosity than Crude Oil A. Nevertheless, the increase or decrease is not significant on the Non-Newtonian viscosity of the emulsion in comparison with the original crude oil at WAT.

TABLE 16. Viscosity of Emulsions and CRUDE A at WAT

Sample	WAT (°C)	Viscosity (Pa.s)
A	41.342	0.0196006
B	41.169	0.0179952
C	40.436	0.0209256
D	40.468	0.0155135
CRUDE OIL A	≈39	0.0183402

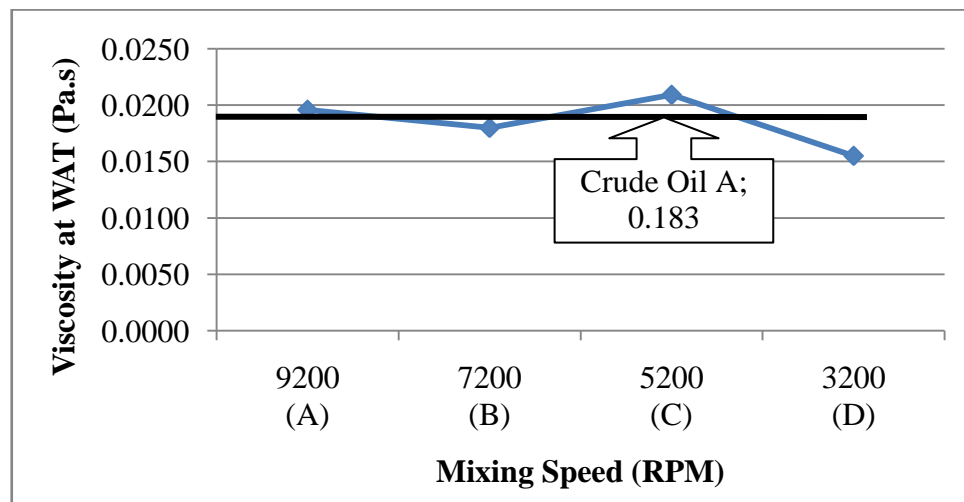


FIGURE 9. Viscosity at WAT against Mixing Speed for Emulsions formed at 60°C and Crude Oil A

ii) Viscosity above WAT

The viscosity values above WAT was analysed to obtain a model for each emulsion sample including Crude Oil A. According to Goh (2010), the effect of temperature on viscosity is commonly explained using the Arrhenius-type relationship:

$$\eta = \eta_0 e^{\frac{E_a}{RT}}$$

Where,  $\eta$  = dynamic viscosity (Pa.s)

$\eta_0$  = viscosity at reference temperature (Pa.s)

$E_a$  = temperature coefficient for viscosity (J/mol)

R = gas constant (J/mol/K)

T = absolute temperature (K)

The same model is used to analyse the viscosity of the emulsion. The model equations for all samples are shown in the table below. From the flow temperature ramp graph, it is observed that only Emulsions A and B as well as Crude Oil A obey the Arrhenius model where fluid viscosity increase as temperature decrease. The hypothesis of this phenomenon is that the emulsion separation effect of Emulsions C and D is larger than or equal to the Arrhenius effect hence the Arrhenius effect is overshadowed. As separation of emulsion occurs, the viscosity is reduced, hence despite the decrease in temperature that will increase the viscosity (according to Arrhenius model), the viscosity is observed to be constant or increasing; defying the Arrhenius model. Generally, the range of viscosity between emulsions and Crude Oil A above WAT does not reflect any significant difference.

TABLE 17. Model Equation for Viscosity above WAT

Sample	Model Equation
Crude Oil A	$\eta = 3.67833e^{-8} e^{\frac{4128.96}{RT}}$
A	$\eta = 1.79818e^{-5} e^{\frac{2206.23}{RT}}$
B	$\eta = 6.90539e^{-4} e^{\frac{1038.43}{RT}}$
C	$y = 0.045x^{-0.17}$
D	$y = 0.019x^{-0.11}$

### 4.2.3 Yield Stress

#### a) Amplitude Sweep

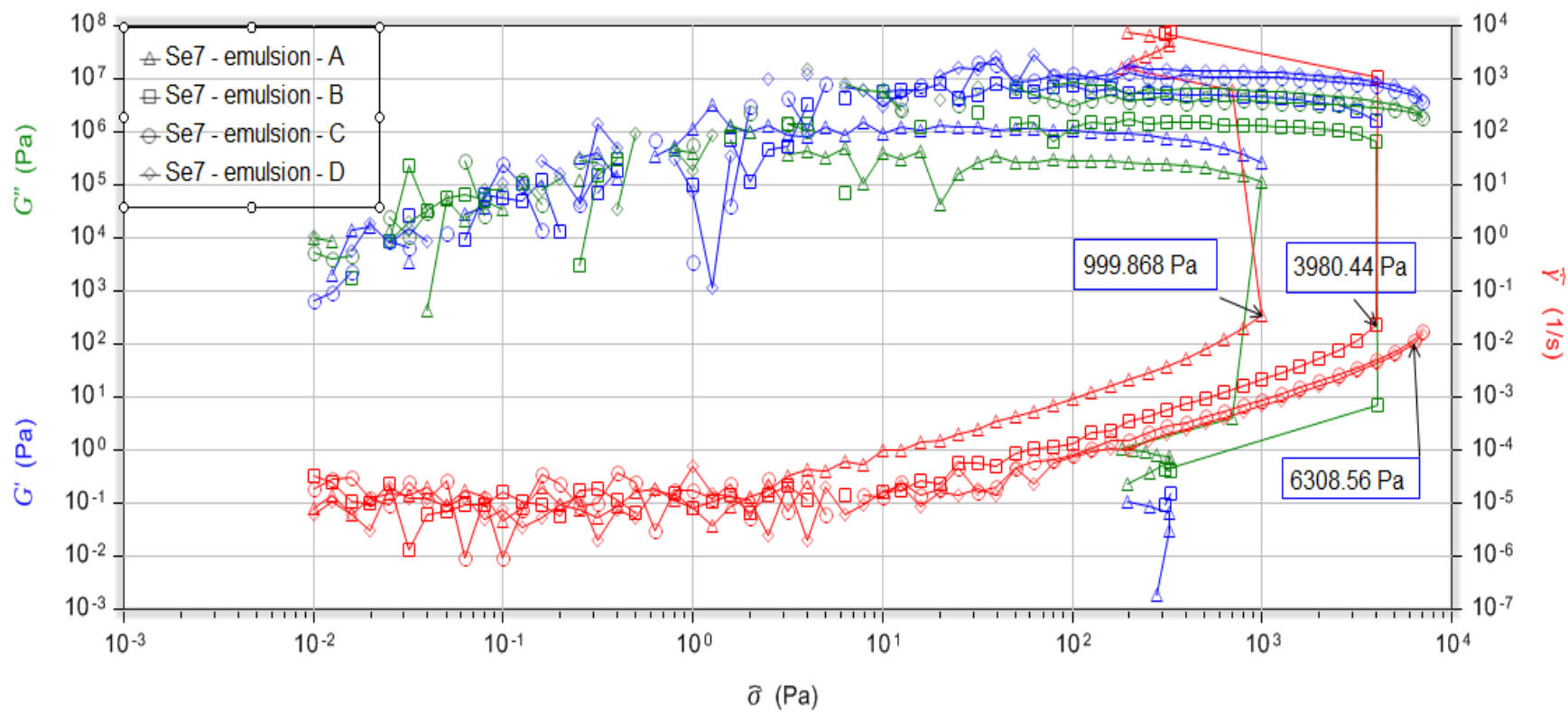


FIGURE 10. Amplitude Sweep Results from Rheological Test

The amplitude sweep experiment was carried out at 20°C and angular frequency of 10.0 rad/s. The oscillation stress was varied from 0.01 to 7000.00 Pa. From this experiment, the yield stress of the emulsions was obtained. Typically, two types of yield stresses can be obtained, first is the yield stress at the point in between the elastic and plastic region and the second is between the plastic and viscous region. In this study, only the first yield stress which is the point where the fluid transitions from the elastic to plastic region is determined. This yield stress is determined at the point where the relationship between the oscillation stress and oscillation strain are no longer linear. The yield stress computed from all the experiments are listed in the table below.

TABLE 18. Yield Stress of Emulsions and Crude Oil A

Sample	Yield Stress (Pa)
Crude Oil A	527.300
A	999.868
B	3980.44
C	6308.56
D	6308.56

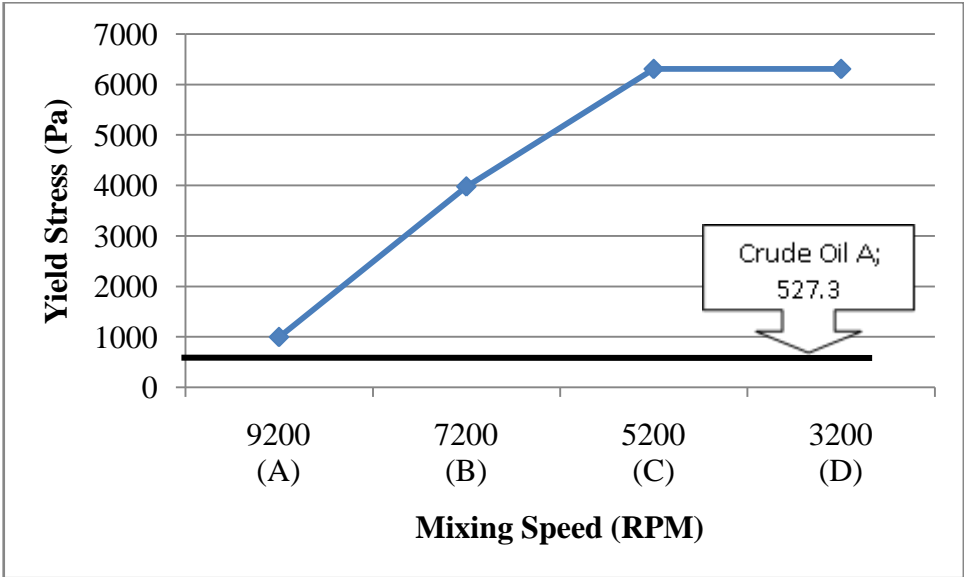


FIGURE 11. Yield Stress against Mixing Speed for Emulsions formed at 60°C and Crude Oil A

All the emulsions increased the yield stress of crude oil and the maximum yield stress is recorded at the lower mixing speeds of 3200 and 5200RPM (Emulsion C and D). Generally, it is observed that the yield stress trend increase as speed decrease and reaches a plateau at lower mixing speeds.

### 4.3 Emulsion Stability

The stability of emulsion was studied using the bottle test. As previously stated, the bottle test was conducted for one month with readings taken every 5<sup>th</sup> minute, 15<sup>th</sup> minute, 30<sup>th</sup> minute, 1<sup>st</sup> hour, 2<sup>nd</sup> hour, 4<sup>th</sup> hour, day 1 until day 7 subsequently week 2, week 3 and week 4. The bottle test will indirectly indicate the tightness of the emulsion; i.e. the longer the time taken to fully separate the emulsion, the higher the stability of the emulsion.

As this study focuses on unresolved emulsion layer (rag layer), the layer volume and thickness is used as an indicator of the emulsion stability. The duration needed for the rag layer to reach a stable volume (no changes in rag layer volume) is the measurement used to categorize the stability of the rag layer.

#### 4.3.1 Crude A

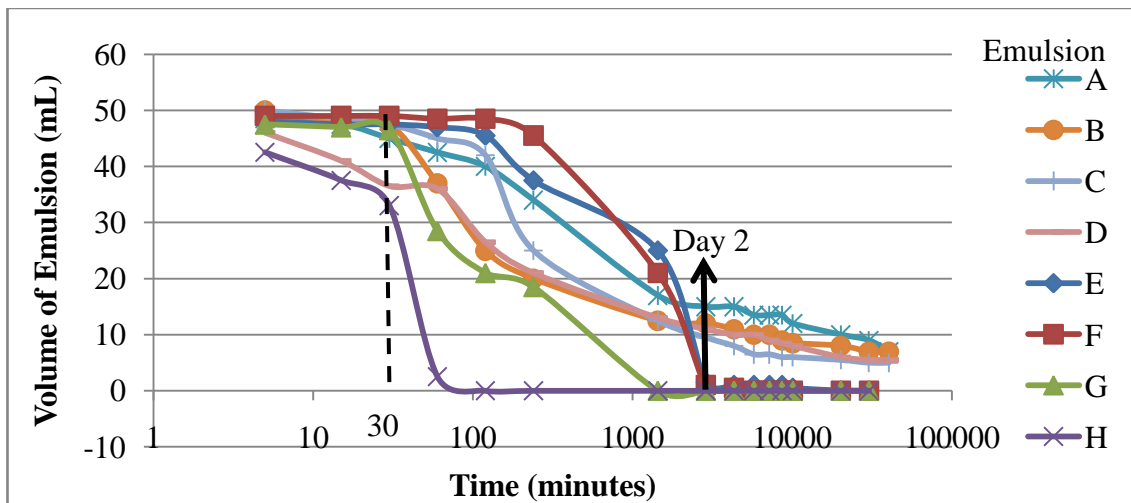


FIGURE 12. Reduction of Volume of Emulsion of CRUDE A at 60°C and 80°C

In Figure 12, the time taken for the volume of emulsion layer to separate is analysed for emulsions of Crude A at 60°C and 80°C. From the graph, it is observed that at 60°C, the emulsion layer is still present at the end of the one month observation and is known as the rag layer. This phenomenon is not seen in the 80°C experiments which imply that for emulsions formed at 80°C, emulsion stability is not a major concern. The rate of reduction of Emulsions E, F, G, and H is noticeably higher than that of Emulsions A, B, C, and D as identified by the ability of Emulsions E, F, G, and H to separate completely by Day 2. Also observed, all emulsions start separating immediately although the rate of separation may be very low except Emulsions B and C that starts separating only in the 15<sup>th</sup> minute.

Construing from the data obtained, a higher temperature provides higher energy for the oil and water droplets to move and hence increase the interaction between each molecules. This encourages the droplets in the emulsion to flocculate or coalesce to its individual phases. Through these processes, the droplets will allow sedimentation and creaming to take place for a successful separation of the emulsion hence the complete separation of emulsion at 80°C.

A further observation on the data above shows that as mixing speed increase, the time taken for the emulsion to separate also increase regardless of temperature. This indicates that the stability of emulsion increases with higher mixing energy. From section 4.5, smaller water droplets are produced in the rag layer with higher mixing speed therefore increasing the difficulty for separation of phases to occur. In spite of this, at 60°C, emulsion mixed with 5200RPM (Emulsion C) shows lower stability than emulsion mixed with 3200RPM (Emulsion D).

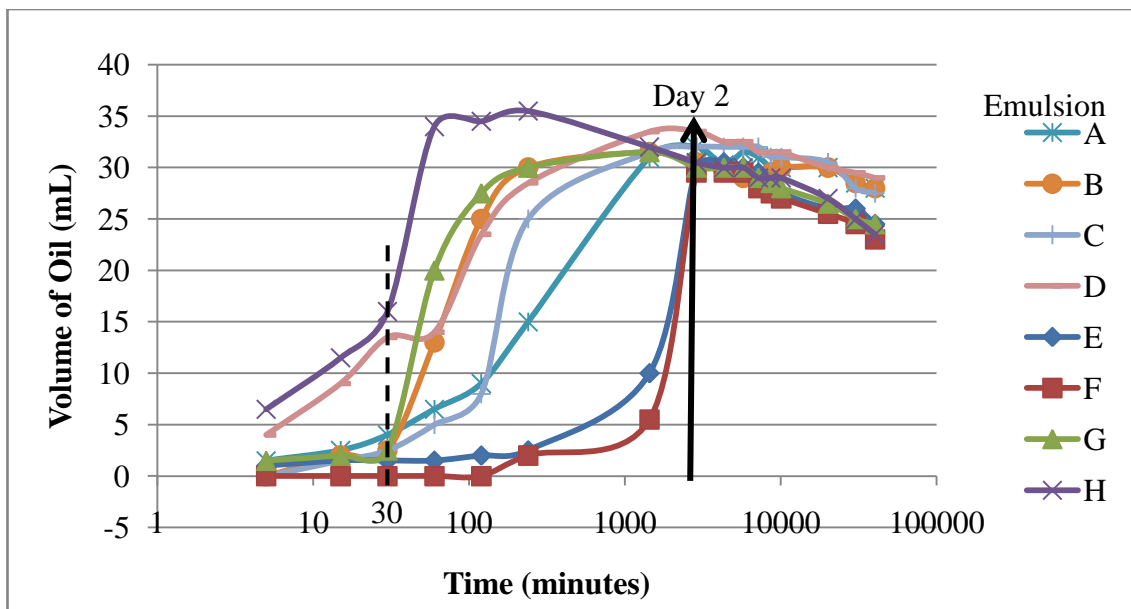


FIGURE 13. Total Volume of Oil Layer of CRUDE A at 60°C and 80°C

Figure 13 shows the change in the volume of oil during bottle test. As early as the 5<sup>th</sup> minute, the oil in the emulsion started to separate into its phase, except for the data scatter produced by mid range speed, a trend of extremely high and extremely low speed is detected. For example, at both low and high mixing temperature, oil separate faster at low mixing speed. It is gathered that the middle range mixing speed of 7200 and 5200 RPM imposed “tighter” emulsion and subsequently cause a delay in initiating the separation process of the oil layer from the emulsion as well as a lower rate of separation. The lowest mixing speed proves to be the easiest to separate. The decrease in oil volume towards the end of the bottle test is associated to the loss in volume due to the presence of heat where a significant loss of lower-boiling-point hydrocarbon may occur.

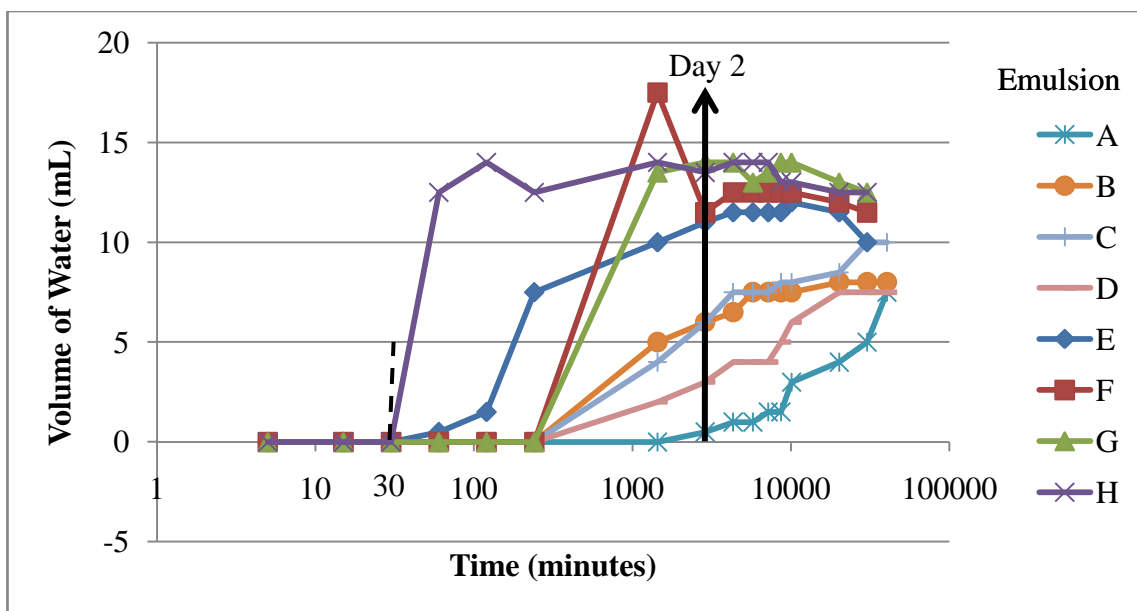


FIGURE 14. Total Volume of Water Layer of CRUDE A at 60°C and 80°C

The separation of the water layer took a longer time to begin as compared to the oil layer. An outlier is identified in Emulsion F, although there is a large volume of water at Day 1, this water layer was very cloudy and may still contain a high concentration of oil. The trend showed that water phase separates faster for emulsion mixed at higher temperature due to the low viscosity of the continuous phase (oil) and high thermal energy that facilitate diffusion process of water droplets.

Inferentially, the rate of separation of oil is higher than water or in other words there are two steps of separation process as reflected in Figures 13 and 14. This indicates that oil can be separated faster from the emulsion as compared to water. Oil is seen to take a shorter time to reach its maximum separation volume while water takes a longer time. However, this does not denote higher water content trapped in the rag layer formed after the one month observation period instead it only shows that at some point of time during the separation process, the water fraction in the emulsion layer is higher than the initial emulsion. Majority of the emulsions begin water separation only after the 4<sup>th</sup> hour with Emulsion A starting the latest (after Day 1).

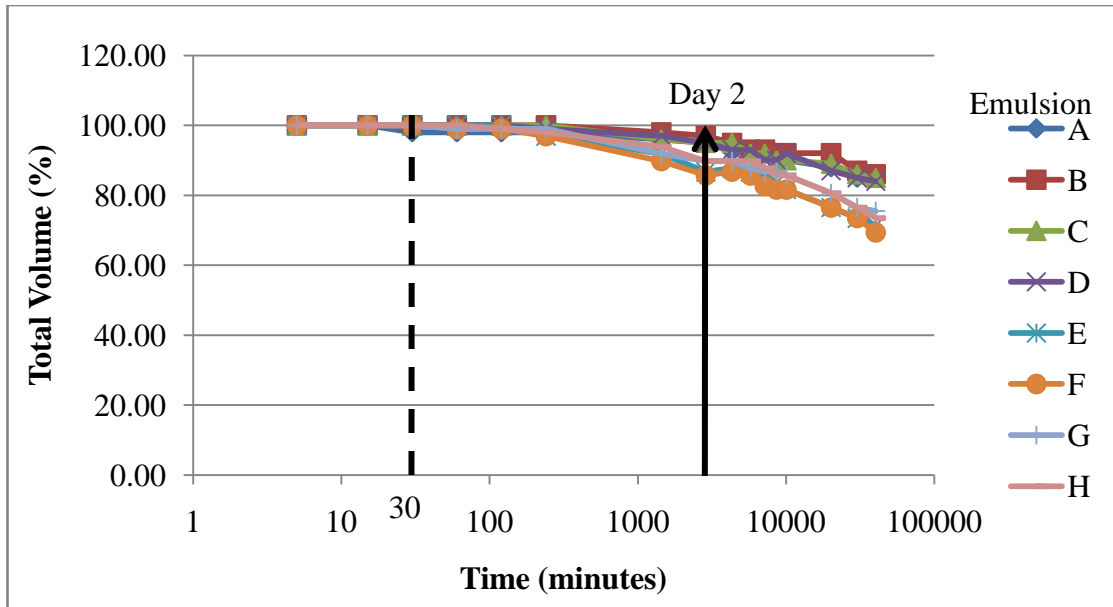


FIGURE 15. Total Volume of Sample in Percentage of CRUDE A at 60°C and 80°C

The total volume of emulsion decreases with time and is consistent with both temperature and mixing speed. According to Smith and Arnold (1987), the addition of heat to well fluids may cause significant losses of the lower-boiling-point hydrocarbons which will result in the loss of volume of the oil. Hence, the phenomenon of decreasing total volume is explained. This is further proven by experiments carried out at 60°C and 80°C to study on the evaporation rate of oil and water. The figures below shows the volume of oil and water without mixing observed at both 60°C and 80°C for one month. It is observed that the loss in volume is greatly contributed by the loss of oil volume due to high temperature.

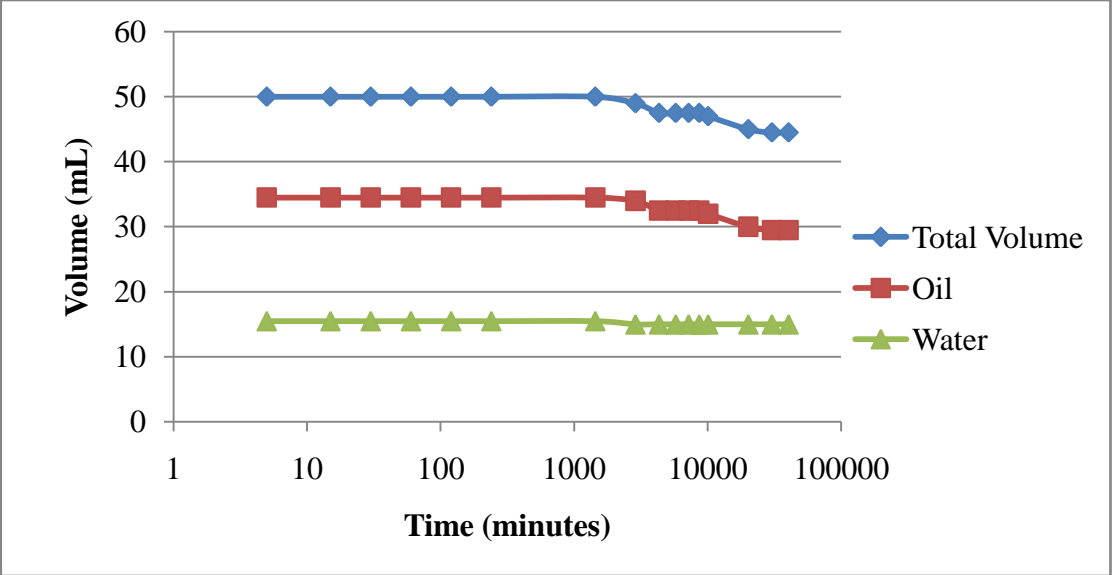


FIGURE 16. Rate of evaporation of Oil and Water at 60°C

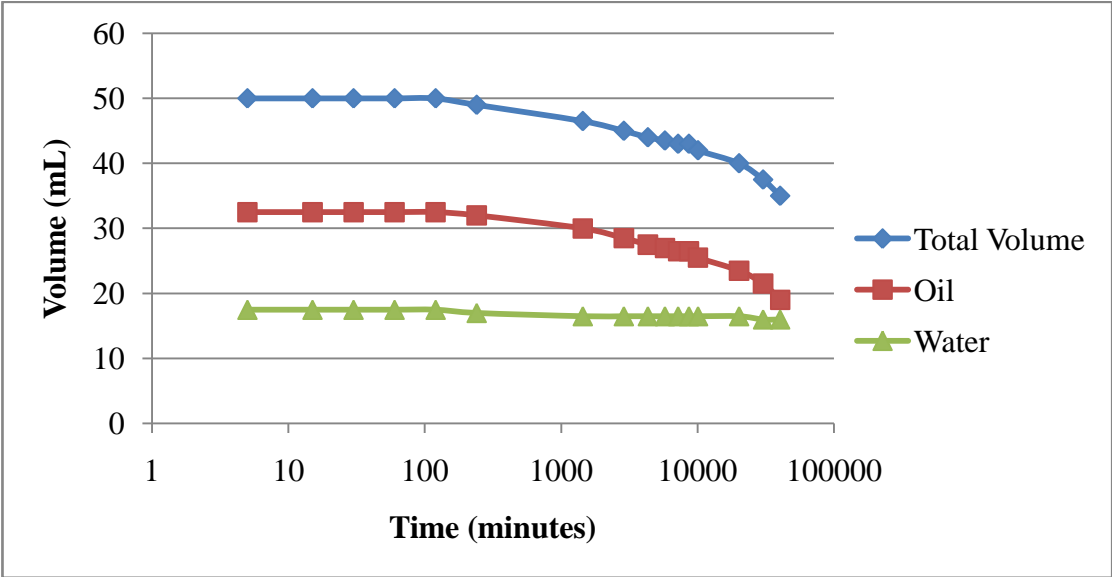


FIGURE 17. Rate of evaporation of Oil and Water at 80°C

From the analysis carried out thus far, Emulsion H has been identified as the least stable emulsion with mixing parameters of 80°C and 3200RPM while the most stable is Emulsion A with mixing parameters of 60°C and 9200RPM. An inconsistency has also been spotted for emulsions at mixing speed of 7200 and 5200RPM.

a) Crude A at 60°C

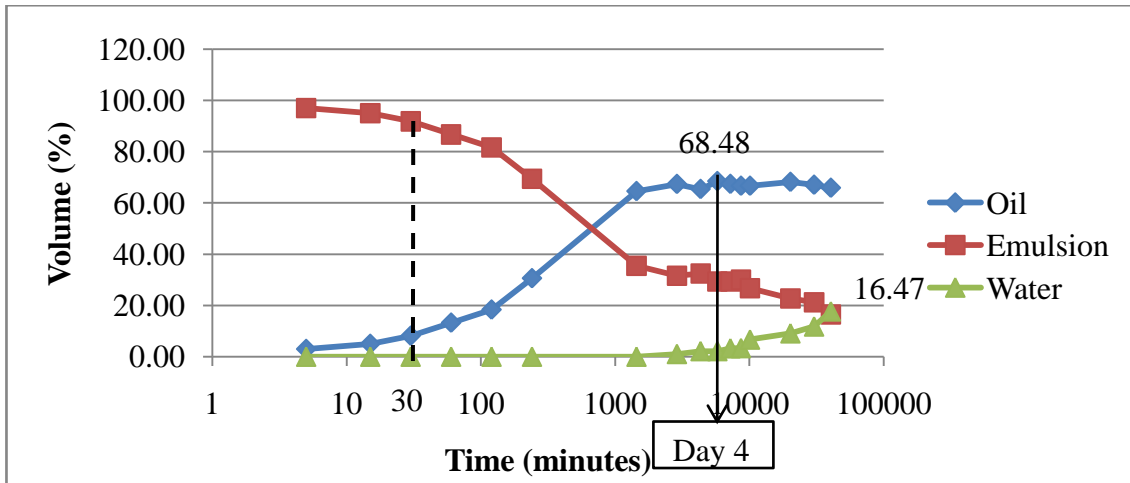


FIGURE 18. Volume of Layers in Percentage of Experiment A

As observed in the graph above, the separation of oil started from the 5<sup>th</sup> minute. The separation of oil begins earlier than water. A sudden acceleration of oil separation is seen after the 4<sup>th</sup> hour. The most active period of emulsion reduction for Experiment A is from the 4<sup>th</sup> hour to Day 1. At Day 1, sixty over percent of oil from the emulsion has been recovered. The final percentage of rag layer volume is 16.5%. From the water content data obtained, in the 16.5% of rag layer, the ratio of oil to water is approximately 74:26.

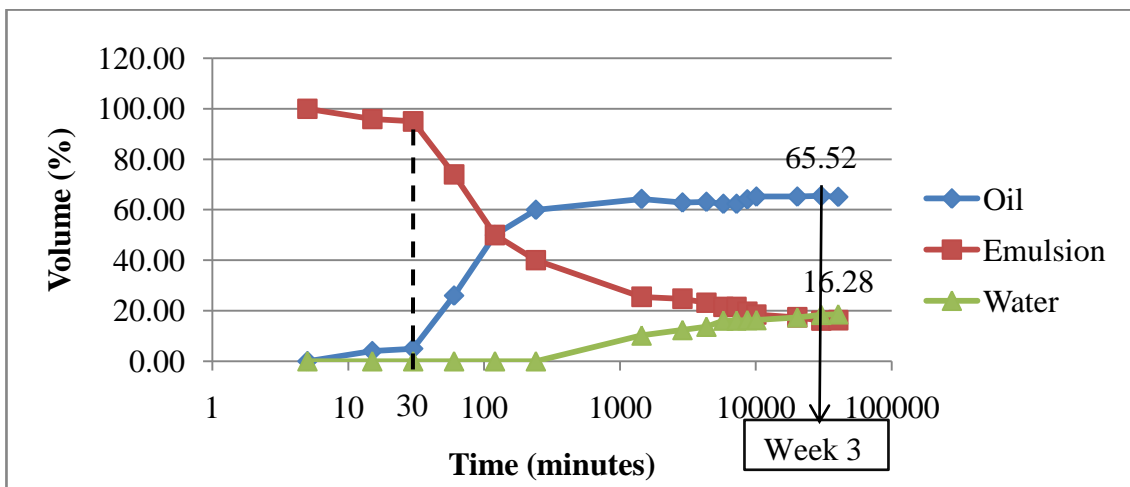


FIGURE 19. Volume of Layers in Percentage of Experiment B

The separation of Emulsion B only started taking place after the first 5 minutes with the oil separating first. A large percentage of oil separation took place between the 1<sup>st</sup> and 2<sup>nd</sup> hour. Up to three weeks was taken to recover the maximum percentage of oil of 65.52%. After the one month observation period, the percentage of rag layer volume is at 16.28%. From the titration test, the water content in the rag layer is about 32.5%.

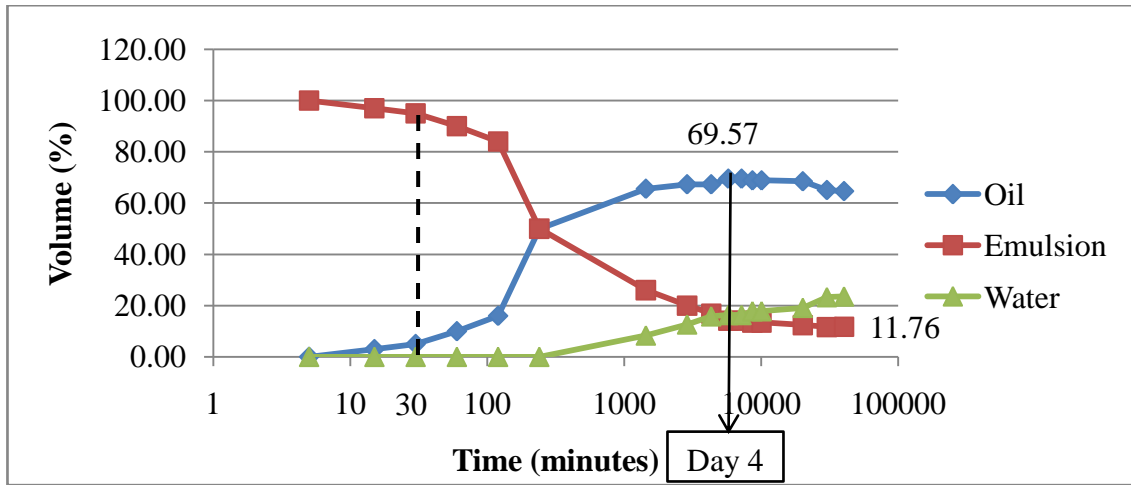


FIGURE 20. Volume of Layers in Percentage of Experiment C

From Figure 20, the separation process of Emulsion C started after the 5<sup>th</sup> minute. A sudden spike in the volume of oil layer is observed between the 2<sup>nd</sup> and 4<sup>th</sup> hour. The maximum percentage of oil recovery is 69.57% and it took four days to reach this level. At week 4, the percentage of rag layer volume is 11.76% and in the rag layer about 33% is made up of water as observed in the titration results.

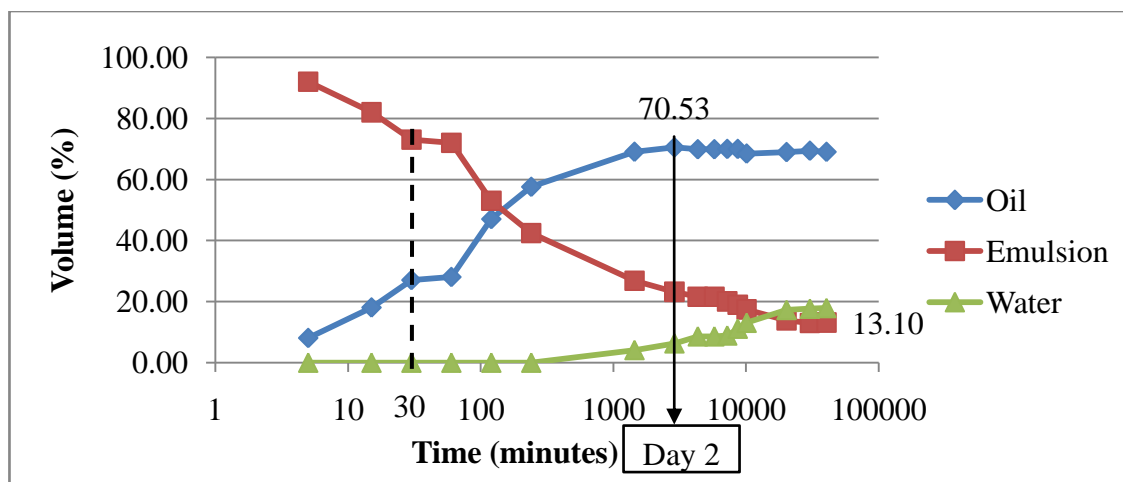


FIGURE 21. Volume of Layers in Percentage of Experiment D

The separation process of Emulsion D begins from the first five minutes of observation as seen in the figure above. The biggest leap in oil volume occurred between the 1<sup>st</sup> and 2<sup>nd</sup> hour. At Day 2 the oil separation volume reached its peak. The percentage of oil in the emulsion is observed to be slightly higher than the mixing ratio of 30:70. This condition may have occurred due to the low sensitivity of equipments used or due to the indistinguishable oil/emulsion interface. The final percentage of rag layer volume is 13.1%. From the water content data obtained, in the 13.1% of rag layer, the ratio of oil to water is approximately 66:34.

Among the emulsions formed at 60°C, Emulsion B that was mixed with a speed of 7200RPM took the longest time to separate to its maximum volume percentage while the fastest was Emulsion C which was mixed at 5200RPM. A higher mixing speed is known to produce smaller droplets of water and oil that makes it more difficult for sedimentation or creaming to occur hence prohibits emulsion separation. From the analysis carried out, the difficulty in separation is directly proportional to the mixing speed except for the middle range speed where an inconsistent trend is observed. No complete separation has been observed in all emulsions which indicate that emulsions formed at 60°C have rag layer issues. The percentage of rag layer volume is below 20% for all emulsions. At very high speed the stability is high while at very low speed the stability is low.

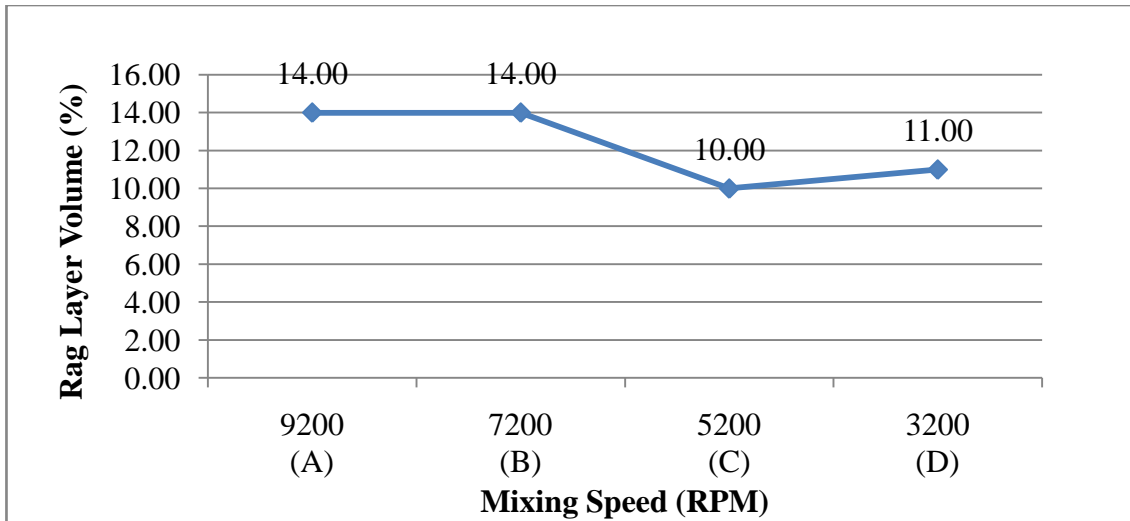


FIGURE 22. Rag Layer Volume in Percentage against Mixing Speed for Emulsions at 60°C

Comparing the highest and lowest mixing speed, it is observed that the highest mixing speed produces a higher percentage of rag layer volume than that of the lower mixing speed. Inconsistency in the middle range speed is yet again detected.

**b) Crude A at 80°C**

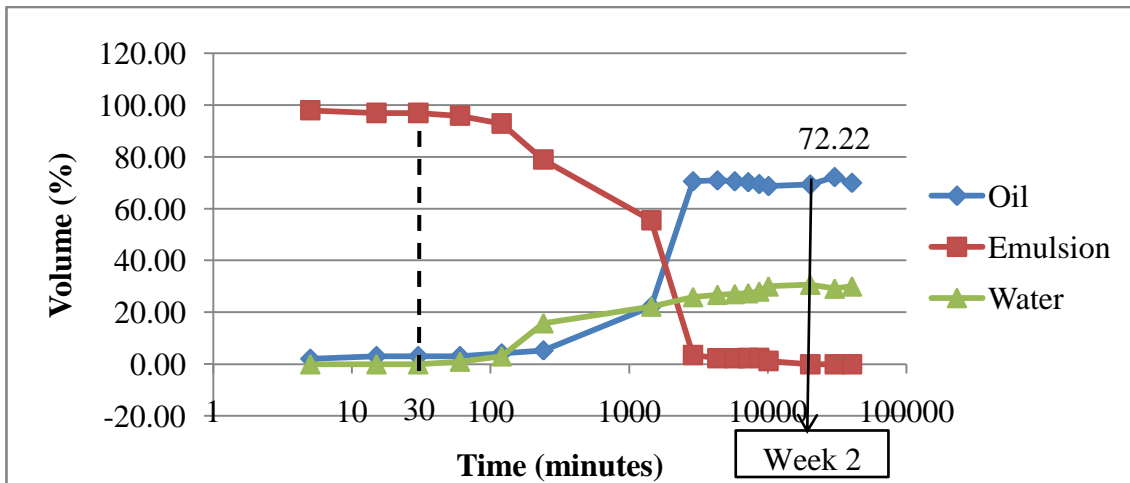


FIGURE 23. Volume of Layers in Percentage of Experiment E

From the graph above, the separation of oil is observed from the 5<sup>th</sup> minute. The separation of oil is observed to have begun earlier than water. A sudden acceleration of oil separation is seen after Day 1. The maximum percentage of oil recovered is 72.2% at Week 3. Although the maximum percentage of oil recovery happens only at Week 3, at week 2 emulsions is no longer observed. This situation may occur when the emulsion layer is too small and the oil/water interface is indistinguishable.

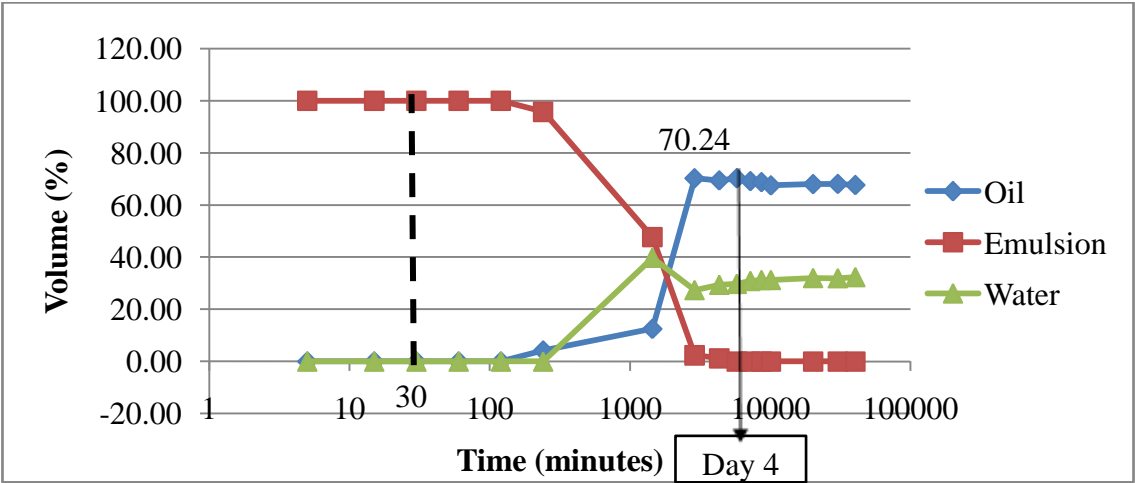


FIGURE 24. Volume of Layers in Percentage of Experiment F

Emulsion F started separating only after the 2<sup>nd</sup> hour, this indicates a fairly tight emulsion. The largest separation percentage is observed between Day 1 and Day 2. The maximum percentage of oil recovery occurs at Day 2. From Day 4 onwards, no emulsion is observed which suggest that all the oil has been separated.

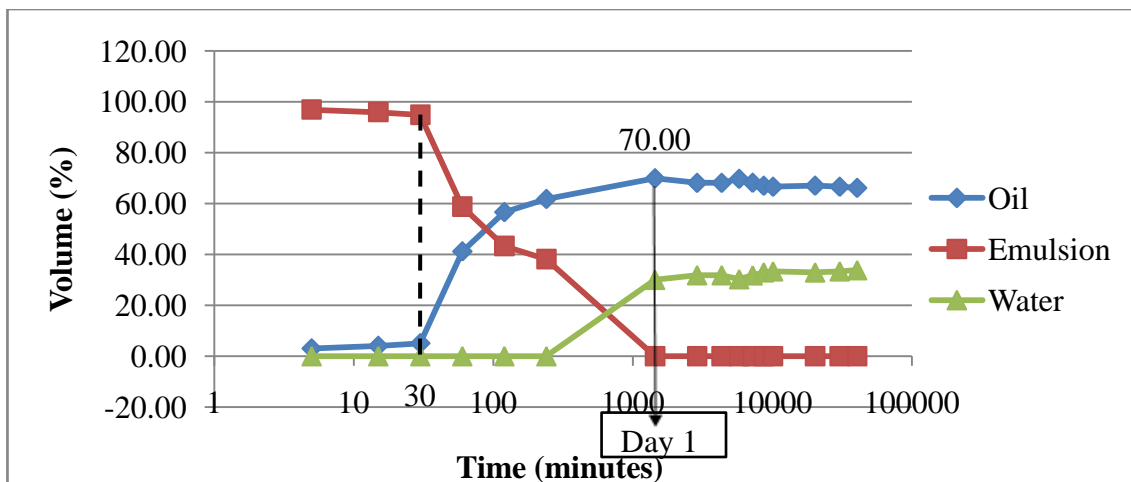


FIGURE 25. Volume of Layers in Percentage of Experiment G

The separation process of Emulsion G takes place from the 5<sup>th</sup> minute. The largest separation occurs between the 30<sup>th</sup> minute and 1<sup>st</sup> hour. The maximum oil recovery is 70% and suggests that all the oil in the emulsion has been separated. This is further supported by the emulsion data which shows that no emulsion is present from Day 1 onwards.

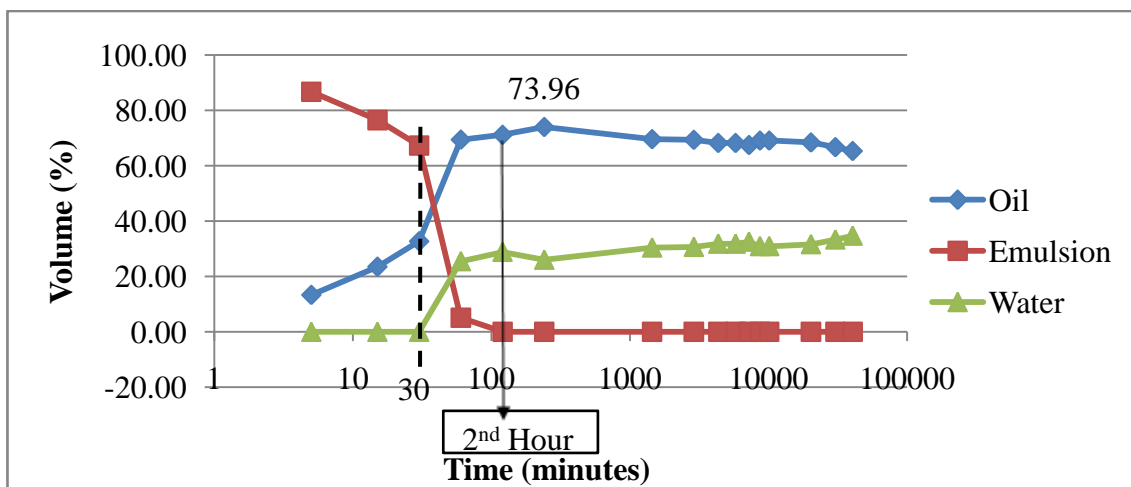


FIGURE 26. Volume of Layers in Percentage of Experiment H

Analyzing Figure 26, the emulsion started separating from the 5<sup>th</sup> minute. Between the 30<sup>th</sup> minute and 1<sup>st</sup> hour there was a large change in the volume of oil. The highest recovery of oil is identified at the 4<sup>th</sup> hour. This observation denotes a high separation rate. No emulsion is observed from the 2<sup>nd</sup> hour onwards.

Emulsion H has the lowest stability at 80°C while Emulsion E is the most stable. Emulsion E took 2 weeks to have complete separation while Emulsion H took only 2 hours to completely separate. A higher mixing speed is known to produce smaller droplets of water and oil that makes it more difficult for sedimentation or creaming to occur hence prohibits emulsion separation. This phenomenon is also observed for emulsion mixed at 60°C. All the emulsions synthesized at 80°C suggest that there are no rag layer issues as no emulsion is observed at the end of the one month observation.

#### **4.3.2 Crude B**

At 60°C, the formation of emulsion using Crude B is observed to produce loose oil-in-water emulsions. There is no water-in-oil emulsion formed during and after the mixing of Crude B with formation water. From observations, the effect of the mixing energy only produces water with different levels of transparency which can be used to identify the varying stability of oil-in-water emulsions. Turbidity is a measurement used to determine the amount of material suspended in water by assessing the water clarity (United States Environmental Protection Agency, 2012). Emulsion stability can then be determined by measuring the turbidity as a function of time (Reddy and Fogler, 1979). Shahin et al. (2011) previously mentioned that the highest turbidity emulsion contains the smallest droplet size and exhibits maximum emulsion stability. Since the exact water content in the oil-in-water emulsion was not measured due to the high separation rate, the level of transparency of the water layer is used to describe the stability of emulsion.

During the first few hours of bottle test, the water is observed to be very cloudy and as time increases the water became less cloudy and more transparent. This phenomenon is observed for all Emulsions I, J, K and L. Nevertheless, despite going

through the same phenomenon, the emulsion that was formed with higher mixing energy (I and J) recorded cloudier emulsion when compared to Emulsions K and L which were formed with lower mixing energy. The cloudiness of the water in the emulsion is recorded using a Likert scale with 1 for not cloudy and 10 for very cloudy.

TABLE 19. Likert Scale Data of Emulsions I, J, K and L

	<b>5th M</b>	<b>15th M</b>	<b>30th M</b>	<b>1st H</b>	<b>2nd H</b>	<b>4th H</b>	<b>D 1</b>	<b>D 2</b>	<b>D 3</b>	<b>D 4</b>	<b>D 5</b>	<b>D 6</b>	<b>D 7</b>	<b>W 2</b>	<b>W 3</b>	<b>W 4</b>
<b>I</b>	10	10	10	9	9	9	7	5	5	5	4	3	3	3	2	1
<b>J</b>	10	10	9	9	9	7	6	5	5	4	3	3	2	2	1	1
<b>K</b>	5	5	4	4	3	2	1	1	1	1	1	1	1	1	0	0
<b>L</b>	4	3	3	3	2	1	1	1	1	1	1	1	1	0	0	0

**M:** Minute **H:** Hour **D:** Day **W:**Week

As observed from the Likert table, Emulsions I and J which were formed using a higher mixing speed of 9200 and 7200RPM have cloudier water as compared to Emulsions K and L which were formed using lower mixing speed of 5200 and 3200RPM. Despite not having water-in-oil emulsion, the effect of the mixing energy can still be observed on the quality of water layer (oil-in-water emulsion).

The emulsions formed using Crude B at 80°C is also observed to produce loose emulsions. No water-in-oil emulsion was identified during and after the mixing of Crude B with formation water. From observations, only oil-in-water emulsions were formed and the effect of different imposed mechanical energy are shown through the varying levels of transparency of the water phase.

During the first few hours of bottle test, the water is observed to be cloudy however the level of cloudiness is lower than that of emulsions mixed at 60°C and as time increases the water quickly became less cloudy and more transparent. This phenomenon is observed for all Emulsions M, N, O and P. Having the same phenomena as of observed in Emulsions I, J, K and L, the emulsions that were formed with higher mixing energy (M and N) is recorded to be cloudier when compared to Emulsions O and P which were formed with a lower mixing energy. Despite the same pattern observed,

the level of cloudiness of the water of Emulsions M, N, O and P is significantly lower than the emulsions mixed at 60°C. The cloudiness of the water in the emulsion is recorded using a Likert scale with 1 for not cloudy and 10 for very cloudy.

TABLE 20. Likert Scale Data of Emulsions M, N, O and P

	<b>5th M</b>	<b>15th M</b>	<b>30th M</b>	<b>1st H</b>	<b>2nd H</b>	<b>4th H</b>	<b>D 1</b>	<b>D 2</b>	<b>D 3</b>	<b>D 4</b>	<b>D 5</b>	<b>D 6</b>	<b>D 7</b>	<b>W 2</b>	<b>W 3</b>	<b>W 4</b>
<b>M</b>	4	4	4	4	4	3	3	2	2	2	2	2	2	2	1	0
<b>N</b>	3	3	3	3	3	2	2	2	1	1	1	1	1	1	1	0
<b>O</b>	3	3	3	3	3	2	1	1	1	1	1	1	1	1	0	0
<b>P</b>	3	3	3	3	3	2	1	0	0	0	0	0	0	0	0	0

**M:** Minute **H:** Hour **D:** Day **W:**Week

Supporting previous observations, emulsions synthesized with higher mixing speed produces cloudier water than those produced with lower mixing speeds of 5200 and 3200RPM which suggests that a more stable oil-in-water emulsion is formed at higher mixing speed supporting the hypothesis by Shahin et al. (2011) that high turbidity emulsion contains small droplet size that exhibits maximum emulsion stability. The magnitude of the effect of mixing energy on emulsions could not be probed on emulsions of Crude B however the effect can still be observed. At 80°C sedimentation is observed to occur at Week 2 onwards. A more thorough and accurate research on the stability of oil-in-water emulsions can be carried out by studying the turbidity of the emulsion using the turbidity meter.

#### 4.4 Water Content (Micro-DSC and Titrator)

The Micro-DSC was used to analyse the water content in the emulsions after mixing. Additionally, the Mettler Toledo V30 Titrator was also used to study the water content in the layers of emulsion after the completion of bottle test. After one month, the emulsion is observed to separate into three distinguishable layers; the oil layer, rag layer (unsettled emulsion) and the water layer.

#### 4.4.1 Emulsion

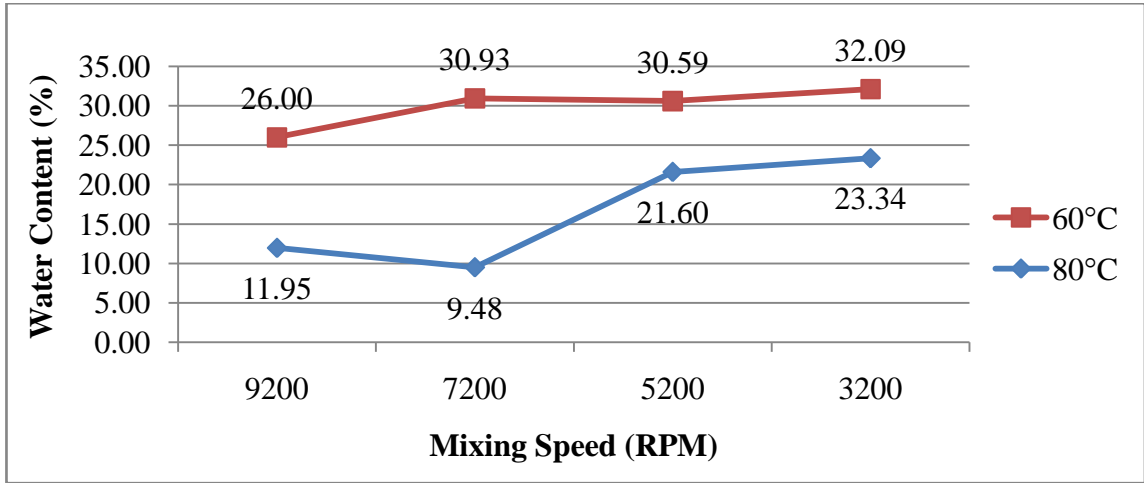


FIGURE 27. Water Content in Emulsion

From the graph above, emulsions formed at 80°C starts separating right after mixing since the water content is lower than its initial fraction of 30%. Emulsions formed at 60°C on the other hand needed some time to begin the separation process. This occurrence was reflected in the study of emulsion stability where emulsions mixed at 80°C started separating first and is less stable than emulsions mixed at 60°C. Since emulsions at 80°C start separating at the early stages, the data above may not reflect the water content accurately as the water content is no longer homogeneous throughout the sample.

#### 4.4.2 Rag Layer

Morvarid (2012) defines rag layer as a layer that prevents complete separation of two fluid phases and hence lowers the overall recovery of oil. The content of water in the rag layer is investigated to study on the percentage of oil and water trapped in the rag layer.

Table 21 below shows the results of rag layer titration for Emulsions A, B, C, and D. There are no significant differences in the water content of the rag layer formed

at different mixing speed. Also observed, the ratio of water and oil in the rag layer is close to the initial water cut of 70:30.

TABLE 21. Oil and Water Composition of Rag Layer

Experiment	Mixing Speed (RPM)	Water Content		Oil Content	
		Weight (g)	Composition (%)	Weight (g)	Composition (%)
A	9200	0.1513	26.16	0.4271	73.84
B	7200	0.1266	32.53	0.2626	67.47
C	5200	0.1258	32.87	0.2570	67.13
D	3200	0.1222	34.10	0.2362	65.90

#### 4.4.3 Oil Layer

Water content in oil layer after the emulsion separation was studied to examine the quality of oil. The most stable emulsion has the highest water content while the least stable emulsion has the lowest water content in the oil layer. This is due to the lower rate of separation of oil and water phases in high mixing energy emulsions and shows a direct relationship between the mixing speed and stability of emulsion. The standard of oil required by the industry should contain water fraction of below 0.5%. Hence, only Emulsion A will require a further treatment.

TABLE 22. Oil and Water Composition of Oil Layer

Experiment	Mixing Speed (RPM)	Water Content		Oil Content	
		Weight (g)	Composition (%)	Weight (g)	Composition (%)
A	9200	0.1774	0.52	33.8725	99.48
B	7200	0.1727	0.18	97.3979	99.82
C	5200	0.2164	0.20	110.1918	99.80
D	3200	0.2172	0.15	141.7436	99.85

#### 4.4.4 Water Layer

The water content in the water layer is used to calculate the content of oil in the water. This step is important to study the quality of water to be discharged. The monthly average oil content of discharge water differs from place to place. In Malaysia, according to the Environmental Quality Act 1974, for standard A quality of water, the oil and grease content should not be detectable while for standard B, is 10mg/l  $\approx$  10ppm  $\approx$  0.001% (Yassin, 1988). Water layer in Emulsions B and D passes the standard A requirement while water from Emulsions A and C do not meet even the standard B requirement. For Emulsions B and D, it is observed that the water content is slightly above 100%, this is probably due to the penetration of moisture from air that affected the measurements during titration.

TABLE 23. Oil and Water Composition of Water Layer

Experiment	Mixing Speed (RPM)	Water Content		Oil Content	
		Weight (g)	Composition (%)	Weight (g)	Composition (%)
A	9200	0.0254	98.48	0.0004	1.52
B	7200	0.0287	100.31	N/A	N/A
C	5200	0.0274	99.23	0.0002	0.77
D	3200	0.0290	100.52	N/A	N/A

## 4.5 Droplet Size

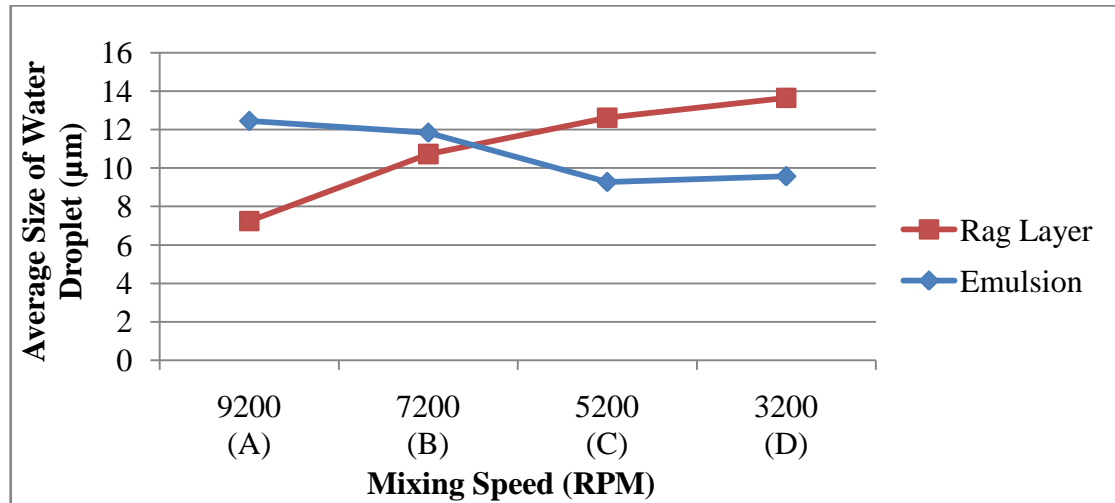


FIGURE 28. Size of Water Droplet in Emulsion and Rag Layer at 60°C

The tabulation of water droplet size in emulsion and rag layer was carried out by obtaining the water droplet distributions from the microscopic images from the Cross-Polarized Microscope.

From the literature review, a higher mixing speed produces smaller water droplets. In the figure above, the size of the water droplet in rag layer is decreasing with increasing speed. The small size of droplets will cause a higher difficulty for creaming to take place and hence increase the stability of the emulsion formed. A smaller water droplet size will inhibit coalescence of the water droplets and slows down the separation process; causing an emulsion to become stable. From previous sections, it is observed that the emulsion with higher mixing speed has a higher stability and supports the information in this section. An opposite trend is however observed for the size of water droplet in emulsion. At higher mixing speed, the size of water droplet in emulsion is observed to be larger and after one month the droplet size decreases. The smaller droplet size observed may be due to the remainder of water droplets that has difficulty in coalescing during the one month period. For the lower mixing speed, as time passes the size of water droplets increase as coalescence of water droplets occur hence forming larger droplets.

#### 4.6 Wax Crystals in Emulsion

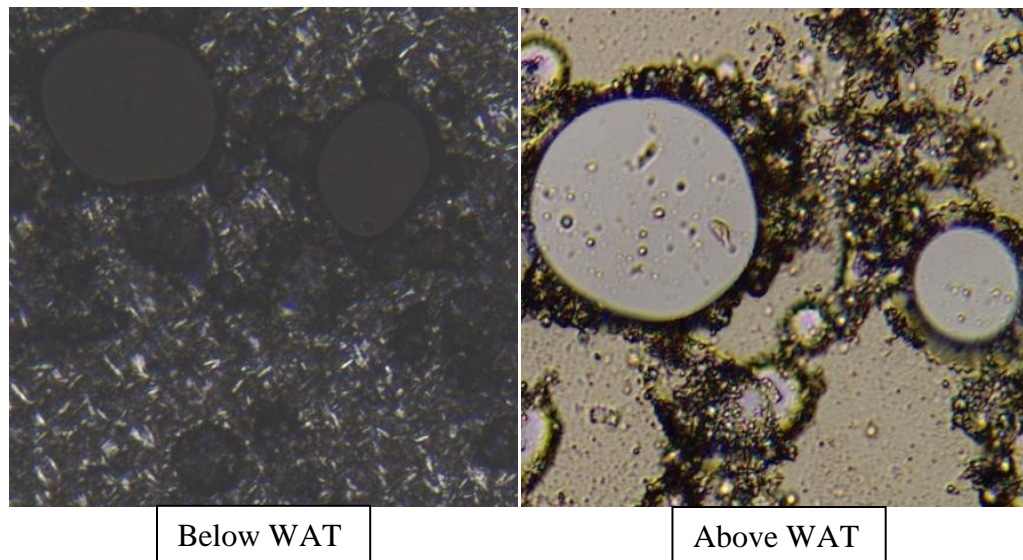


FIGURE 29. Microscopic Image of Wax Crystals for Emulsion A at 33°C (Polarized) and 60°C (Non-Polarized)

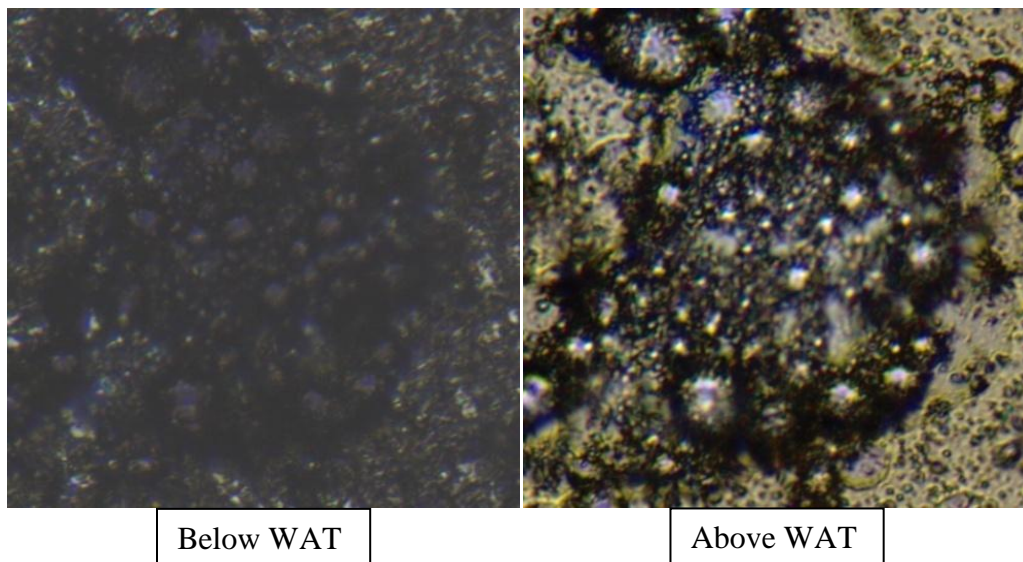


FIGURE 30. Microscopic Image of Wax Crystals for Emulsion B at 33°C (Polarized) and 55°C (Non-Polarized)

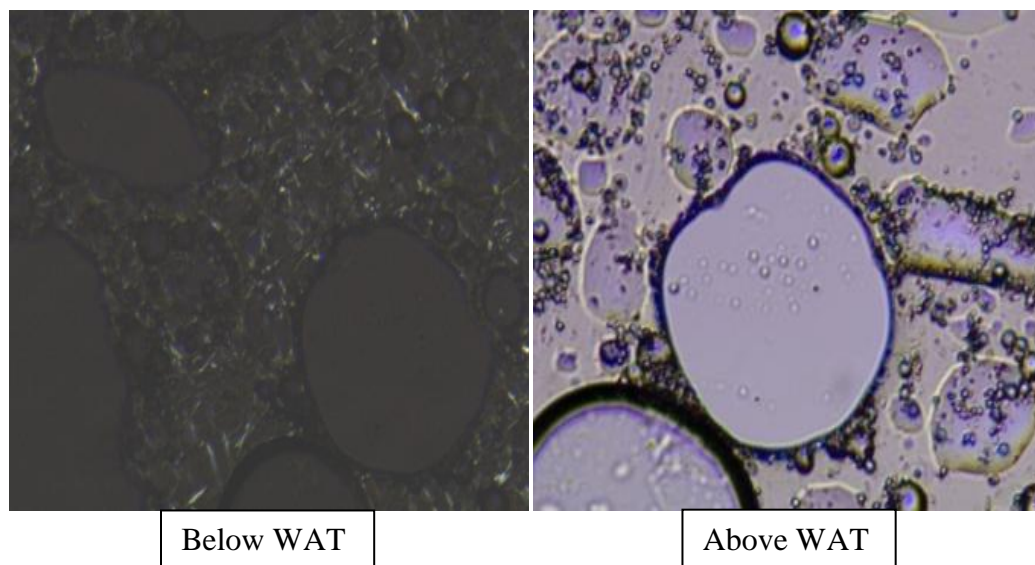


FIGURE 31. Microscopic Image of Wax Crystals for Emulsion C at 33°C (Polarized) and 60°C (Non-Polarized)

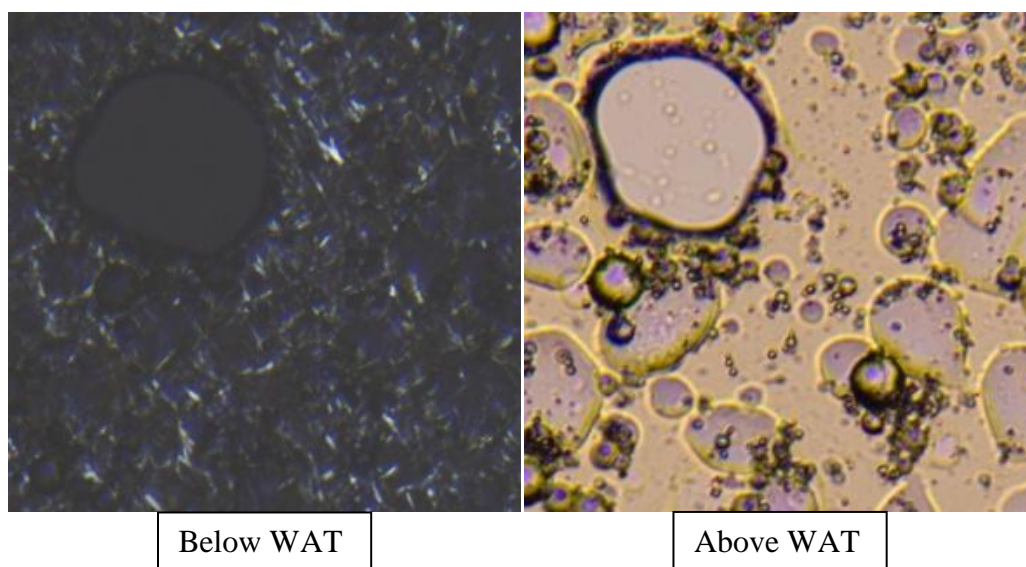


FIGURE 32. Microscopic Image of Wax Crystals for Emulsion D 33°C (Polarized) and 55°C (Non-Polarized)

The images in Figures 29-32 show the microscopic images of the wax crystals at temperatures below and above wax appearance temperature. It is observed that there are more wax crystals surrounding the water droplets at temperature below WAT. At lower temperature, more stable emulsion can be formed due to the physical state of the waxes which are present as fine solids. Above the WAT, there is no wax crystals identified. This occurrence may be due to the change in physical state of the wax that allows coalescence of the droplet to occur more easily. It is observed that there are black coloured interfacial layers on the droplets that prevent coalescence and needs further investigation.

## CHAPTER 5

### CONCLUSION AND RECOMMENDATION

#### 5. CONCLUSION AND RECOMMENDATION

##### 5.1 Conclusion and Future Works

The formation of crude oil emulsion was carried out in the Flow Assurance Laboratory. A study on the oil field environment such as the temperature and flow rate was conducted for parameters selection. The mixing temperatures chosen were 60°C and 80°C. The mixing energy was provided using a homogenizer with four speeds ranging between 9200RPM and 3200RPM.

Comparing Crude A and Crude B, Crude A produces water-in-oil emulsion while Crude B produces oil-in-water emulsion at both 60°C and 80°C. Crude B separates immediately hence do not form water-in-oil emulsion. At 60°C, Crude A produce emulsions that are more stable than emulsions formed at 80°C. Since more stable emulsions are formed at 60°C, these emulsions tend to form rag layer. Emulsions formed at a higher temperature have a higher tendency to separate as compared to the lower temperature emulsion. The WAT of the emulsions were not significantly affected by the mixing temperature with a variance of only  $\pm 1^\circ\text{C}$ .

From the research conducted, emulsions formed with the highest mixing energy have the highest stability while emulsions mixed with the lowest mixing energy are the least stable. The rag layer of emulsion mixed at 9200RPM has the smallest water droplet size and the size of the water droplet increase as the mixing speed decrease. In terms of viscosity, only emulsion formed at higher mixing speeds obey the Arrhenius model above WAT. All the emulsions formed have higher viscosity than pure Crude Oil A at WAT. Also observed is that the highest mixing energy emulsion has a lower yield stress

as compared to the emulsion mixed with the lowest mixing energy. An irregularity is observed for the middle range mixing speeds in terms of water content, viscosity and size of water droplet.

Two identified parameters from this research that should be considered during crude oil extraction are temperature and flow rate. The kinetic energy or the Reynold number should be maintained by controlling the flow rate to have a lower turbulence (mixing) effect in the oil field. Besides the WAT of crude oil as an important parameter in the setting of pipeline environment, the temperature threshold where rag layer forms can be identified to prevent rag layer from forming without forgoing crude oil volume. Through such preventive measures, the demulsification cost of crude oil emulsion can be minimized and losses can be reduced.

This research has been focused on the formation of water-in-oil emulsion. Having said so, a more thorough research can be conducted on the oil-in-water emulsion formed using Crude B. The characteristics of both oil-in-water and water-in-oil emulsion can then be further analysed for a more comprehensive understanding of the relationship between different imposed mechanical energy with rag layer formation and emulsion stability.

## REFERENCES

- Abdel-Raouf, M. E.-S. (2012). Factors Affecting the Stability of Crude Oil Emulsions. In M. E.-S. Abdel-Raouf, *Crude Oil Emulsions- Composition Stability and Characterization* (pp. 183-198). Egypt: InTech.
- Czarnecki, J., Moram, K., & Yang, X. (2007). On the "rag layer" and diluted bitumen froth dewatering. *The Canadian Journal of Chemical Engineering*, 85 , 748-755.
- Ekins, P., Vanner, R., & Firebrace, J. (2005). *MANAGEMENT OF PRODUCED WATER ON OFFSHORE OIL INSTALLATIONS: A COMPARATIVE ASSESSMENT USING FLOW ANALYSIS*. Policy Studies Institute.
- Fingas, M., & Fieldhouse, B. (2003). Studies of the formation process of water-in-oil emulsions. *Marine Pollution Bulletin* , 369-396.
- Gewald, D., Siokos, K., Karellas, S., & Spliethoff, H. (2012). Waste heat recovery from landfill gas-fired power plant. *Renewable and Sustainable Energy Reviews* 16 , 1779-1789.
- Goh, S. E. (2010). The Hidden Property of Arrhenius-type Relationship: Viscosity as a Function of Temperature. *Journal of Physical Science* , 29-39.
- International Association of Oil & Gas Producers. (2002). *Aromatics in produced water: occurrence, fate and effects, and treatment*. London: International Association of Oil & Gas Producers.
- Jimtaisong, A. (2007, December 19). Skin Care Cosmetic Emulsions. Mae Fah Luang University, Thailand.
- Kang, W., Xu, B., Wang, Y., Li, Y., Shan, X., An, F., et al. (2011). Stability mechanism of W/O crude oil emulsion stabilized by polymer and. *Colloids and Surfaces A: Physicochemical and Engineering Aspects* , 565-560.
- Kelesoglu, S., Pettersen, B. H., & Sjoblom, J. (2012). Flow properties of water in North Sea heavy crude oil emulsions. *Journal of Petroleum Science and Engineering* , 14-23.

- Khatri, N. L. (2010). *Measurement and Modeling of Emulsion Layer Growth in Continuous Oil-Water Separations*. Calgary, Alberta: University of Calgary.
- Kokal, S. (2002). Crude Oil Emulsions: A State-Of-The-Art Review. *SPE Annual Technical Conference and Exhibition*. Texas: Society of Petroleum Engineers.
- Kokal, S., & Al-Juraid, J. (1999). *Quantification of Various Factors Affecting Emulsion Stability: Watercut, Temperature, Shear, Asphaltene Content, Demulsifier Dosage and Mixing Different Crudes*. Texas: Society of Petroleum Engineers, Inc.
- Leal-Calderon, F., Schmitt, V., & Bibette, J. (2007). *Emulsion Science*. Springer.
- Morvarid, M. K. (2012). *Study of the Rag Layer: Characterization of Solids*. University of Alberta Libraries.
- Opawale, A., & Osisanya, S. (2013). Tool for Troubleshooting Emulsion Problems in Producing Oilfields. *SPE Production and Operations Symposium*. Oklahoma: Society of Petroleum Engineers.
- Rajalakshmi, R., Mahesh, K., & Ashok Kumar, C. (2011). Retrieved March 10, 2015, from International Journal of Innovative Drug Discovery: [http://www.ijidd.com/File\\_Folder/1-8.pdf](http://www.ijidd.com/File_Folder/1-8.pdf)
- Reddy, S. R., & Fogler, H. S. (1979). *Emulsion Stability: Determination from Turbidity*. Michigan: The University of Michigan.
- Rodionova, G., Pettersen, B., Kelesoglu, S., & Sjoblom, J. (2014). Preparation and Characterization of Reference Fluid Mimicking Behaviour of North Sea Heavy Crude Oil. *Fuel*, 308-314.
- Saadatmand, M., Yarranton, H. W., & Moran, K. (2008). Rag Layers in Oil Sand Froths. *Industrial & Engineering Chemistry Research*, 8828-8839.
- Salleh, L. (2014). *E&P Core Business Process and Environment Case Study*. Tronoh: Universiti Teknologi PETRONAS.

Shahin, M., Abdel Hady, S., Hammad, M., & Mortada, N. (2011). Development of Stable O/W Emulsions of Three Different Oils. *Internation Journal of Phamaceutical Studies and Research* , 45-51.

Slomkowski, S., Aleman, J. V., Gilbert, R. G., Hess, M., Hories, K., Jones, R. G., et al. (2011). *Terminology of Polymers and Polymerization Processes in Dispersed Systems (IUPAC Recommendations)*. Retrieved March 10, 2015, from International Union of Pure and Applied Chemistry: <http://pac.iupac.org/publications/pac/pdf/2011/pdf/8312x2229.pdf>

Smith, H. V., & Arnold, K. E. (1987). Crude Oil Emulsions. In *Petroleum Engineering Handbook* (pp. 19-1-19-34).

Tadros, T. F. (2013). Emulsion Formation, Stability, and Rheology. In T. F. Tadros, *Emulsion Formation and Stability* (pp. 1-75). Wiley-VCH Verlag GmbH & Co. KGaA.

United States Environmental Protection Agency. (2012, March 06). *5.5 Turbidity*. Retrieved April 12, 2015, from United States Environmental Protection Agency: <http://water.epa.gov/type/rsl/monitoring/vms55.cfm>

Varadaraj, R., & Brons, C. (2007). Molecular Origins of Crude Oil Interfacial Activity Part 3: Characterization of the Complex Fluid Rag Layer Formed at Crude Oil-Water Interfaces. *Energy & Fuels*, 21 , 1617-1621.

Yassin, A. A. (1988). Legislation On Oil Pollution Prevention and Control During Petroleum Production. *Journal Teknologi UTM* , 974-984.

## APPENDICES

### Appendix I Calculation of Stirrer Speed of Crude A

#### Pipeline Data

Length of pipeline, D (m)	13600
Pipe inner diameter (m)	0.6096
Pipe inner radius (m)	0.3048
Cross-sectional area of pipe (m <sup>2</sup> )	0.291863508

#### Stirrer Data

Mass of stirrer (kg)	2.5
Radius of arm, R <sub>a</sub> (m)	0.0075

#### CRUDE A

At T<sub>a</sub>=60°C

Volume Flow Rate (bbl/day)	Volume Flow Rate, Q (m <sup>3</sup> /s)	Density (kg/m <sup>3</sup> )	Mass Flow Rate, $\dot{m}$ (kg/s)	Velocity, V (m/s)	Force, F (kg·m/s <sup>2</sup> )	Work, W (kg·m <sup>2</sup> /s <sup>2</sup> )	Mass of Sample (kg)	Stirrer Speed (RPM)
2824	0.005196908	822.92	4.276639823	0.017805955	0.076149654	1035.635298	0.087504692	36023.67084
2303	0.004238130	822.92	3.487642179	0.014520932	0.050643817	688.7559054	0.087504692	29377.66074
1622	0.002984910	822.92	2.456341995	0.010227074	0.025121192	341.6482176	0.087504692	20690.64947
978	0.001799779	822.92	1.481074273	0.00616651	0.009133059	124.2096017	0.087504692	12475.61972

**CRUDE A**At  $T_b=80^\circ\text{C}$ 

<b>Volume Flow Rate (bbl/day)</b>	<b>Volume Flow Rate, Q (m<sup>3</sup>/s)</b>	<b>Density (kg/m<sup>3</sup>)</b>	<b>Mass Flow Rate, <math>\dot{m}</math> (kg/s)</b>	<b>Velocity, V (m/s)</b>	<b>Force, F (kg·m/s<sup>2</sup>)</b>	<b>Work, W (kg·m<sup>2</sup>/s<sup>2</sup>)</b>	<b>Mass of Sample (kg)</b>	<b>Stirrer Speed (RPM)</b>
2824	0.005196908	808.23	4.20029724	0.017805955	0.074790302	1017.148103	0.086138358	35710.12212
2303	0.00423813	808.23	3.425384045	0.014520932	0.04973977	676.4608776	0.086138358	29121.95865
1622	0.00298491	808.23	2.412493669	0.010227074	0.024672752	335.5494324	0.086138358	20510.55881
978	0.001799779	808.23	1.454635517	0.00616651	0.008970024	121.9923278	0.086138358	12367.03238

**Appendix II Calculation of Stirrer Speed of Crude B**

**Pipeline Data**

Length of pipeline, D (m)	13600
Pipe inner diameter (m)	0.6096
Pipe inner radius (m)	0.3048
Cross-sectional area of pipe (m <sup>2</sup> )	0.291863508

**Stirrer Data**

Mass of stirrer (kg)	2.5
Radius of arm, R <sub>a</sub> (m)	0.0075

**CRUDE B**

At T<sub>a</sub>=60°C

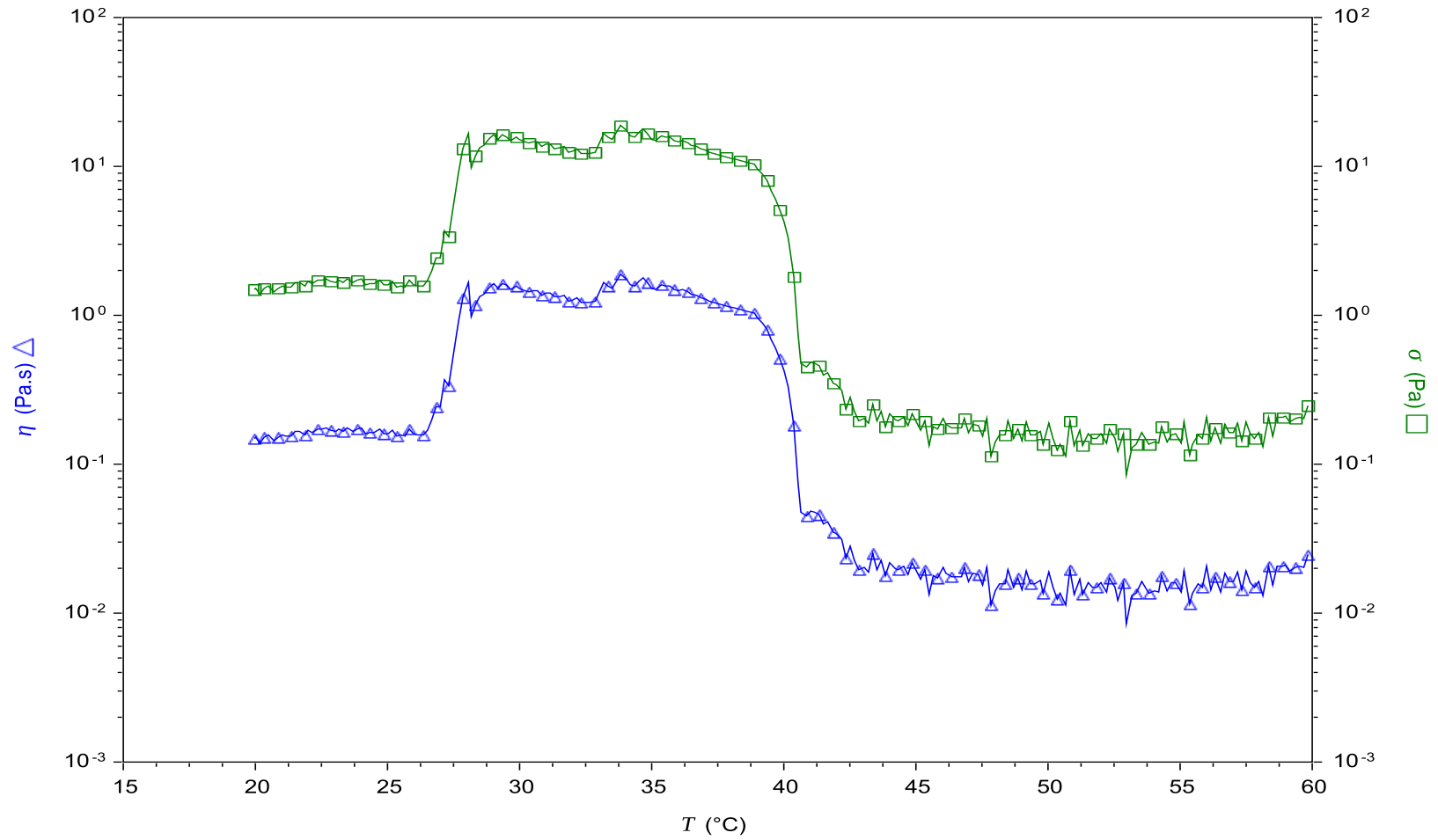
Volume Flow Rate (bbl/day)	Volume Flow Rate, Q (m <sup>3</sup> /s)	Density (kg/m <sup>3</sup> )	Mass Flow Rate, $\dot{m}$ (kg/s)	Velocity, V (m/s)	Force, F (kg·m/s <sup>2</sup> )	Work, W (kg·m <sup>2</sup> /s <sup>2</sup> )	Mass of Sample (kg)	Stirrer Speed (RPM)
2824	0.005196908	835.86	4.343887817	0.017805955	0.077347069	1051.920138	0.088410492	36299.44003
2303	0.00423813	835.86	3.542483585	0.014520932	0.051440165	699.586243	0.088410492	29602.55325
1622	0.00298491	835.86	2.494966728	0.010227074	0.02551621	347.0204627	0.088410492	20849.04098
978	0.001799779	835.86	1.504363416	0.00616651	0.009276672	126.1627348	0.088410492	12571.12335

**CRUDE B**At  $T_b=80^\circ\text{C}$ 

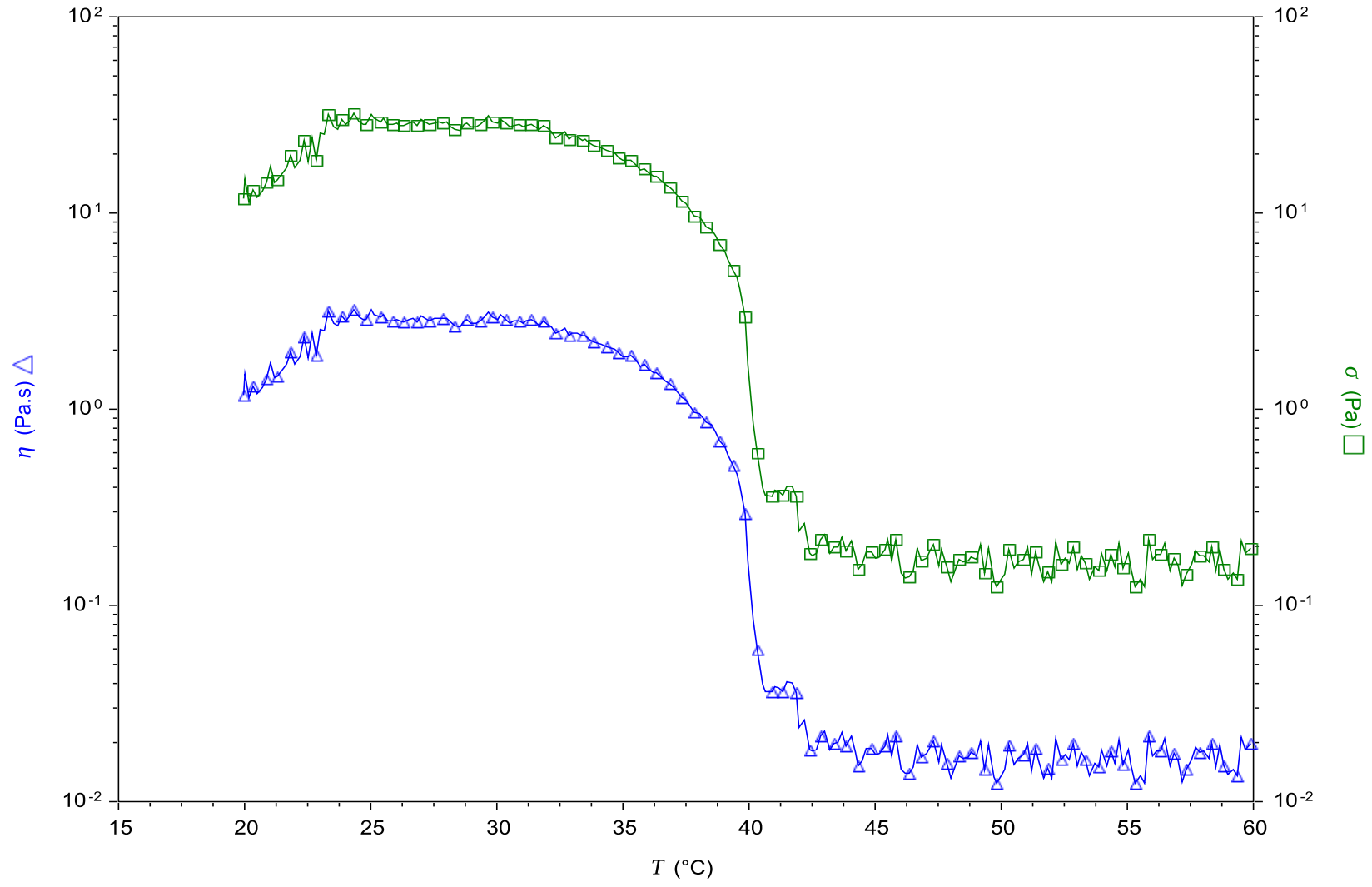
<b>Volume Flow Rate (bbl/day)</b>	<b>Volume Flow Rate, Q (m<sup>3</sup>/s)</b>	<b>Density (kg/m<sup>3</sup>)</b>	<b>Mass Flow Rate, <math>\dot{m}</math> (kg/s)</b>	<b>Velocity, V (m/s)</b>	<b>Force, F (kg·m/s<sup>2</sup>)</b>	<b>Work, W (kg·m<sup>2</sup>/s<sup>2</sup>)</b>	<b>Mass of Sample (kg)</b>	<b>Stirrer Speed (RPM)</b>
2824	0.005196908	821.38	4.268636584	0.017805955	0.076007149	1033.697226	0.087058858	35993.04896
2303	0.00423813	821.38	3.481115458	0.014520932	0.050549043	687.466978	0.087058858	29352.6883
1622	0.00298491	821.38	2.451745234	0.010227074	0.025074181	341.0088623	0.087058858	20673.06141
978	0.001799779	821.38	1.478302613	0.00616651	0.009115967	123.9771577	0.087058858	12465.01483

# Appendix III Rheometer results of Flow Temperature Ramp

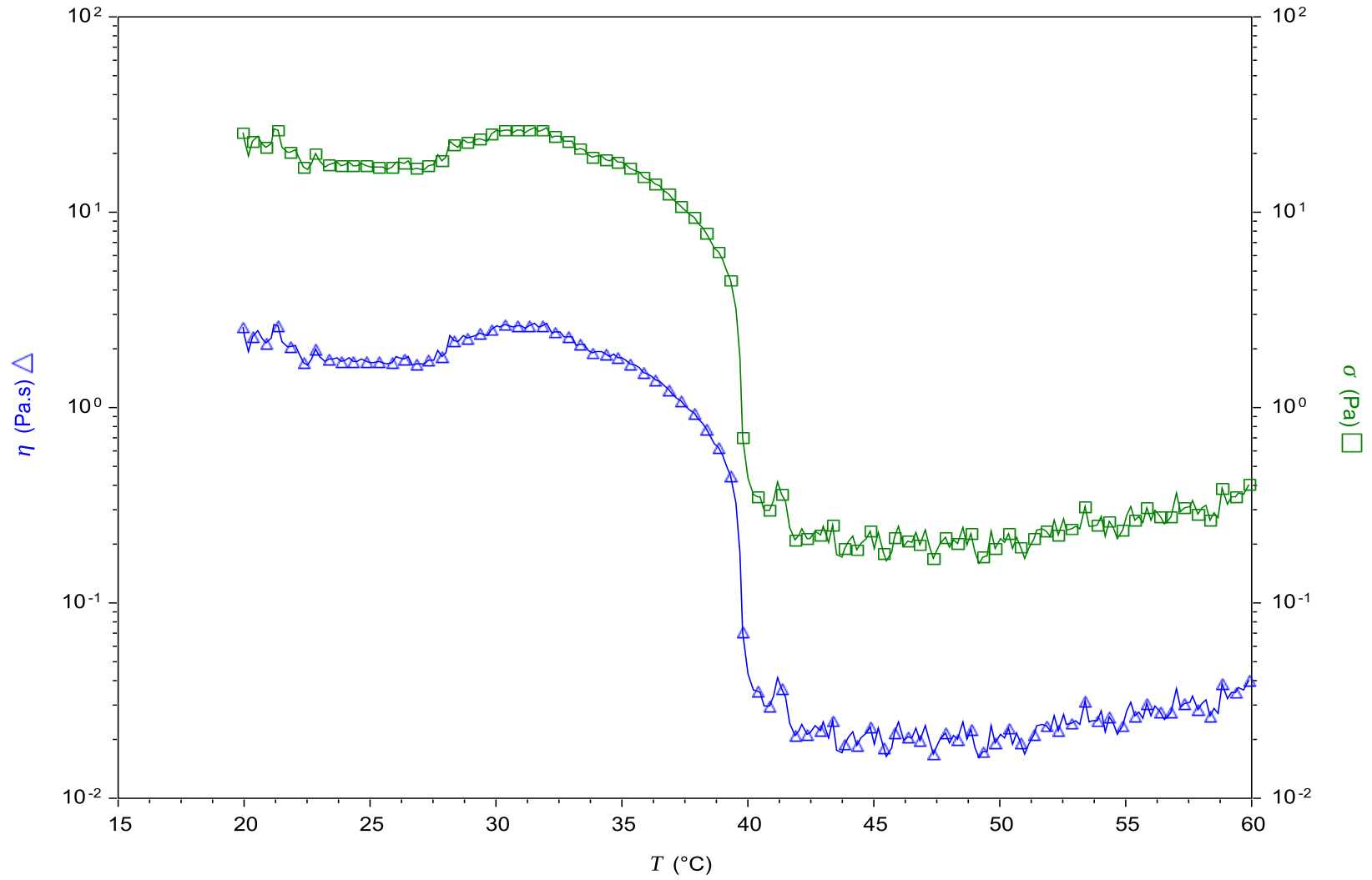
## Emulsion A



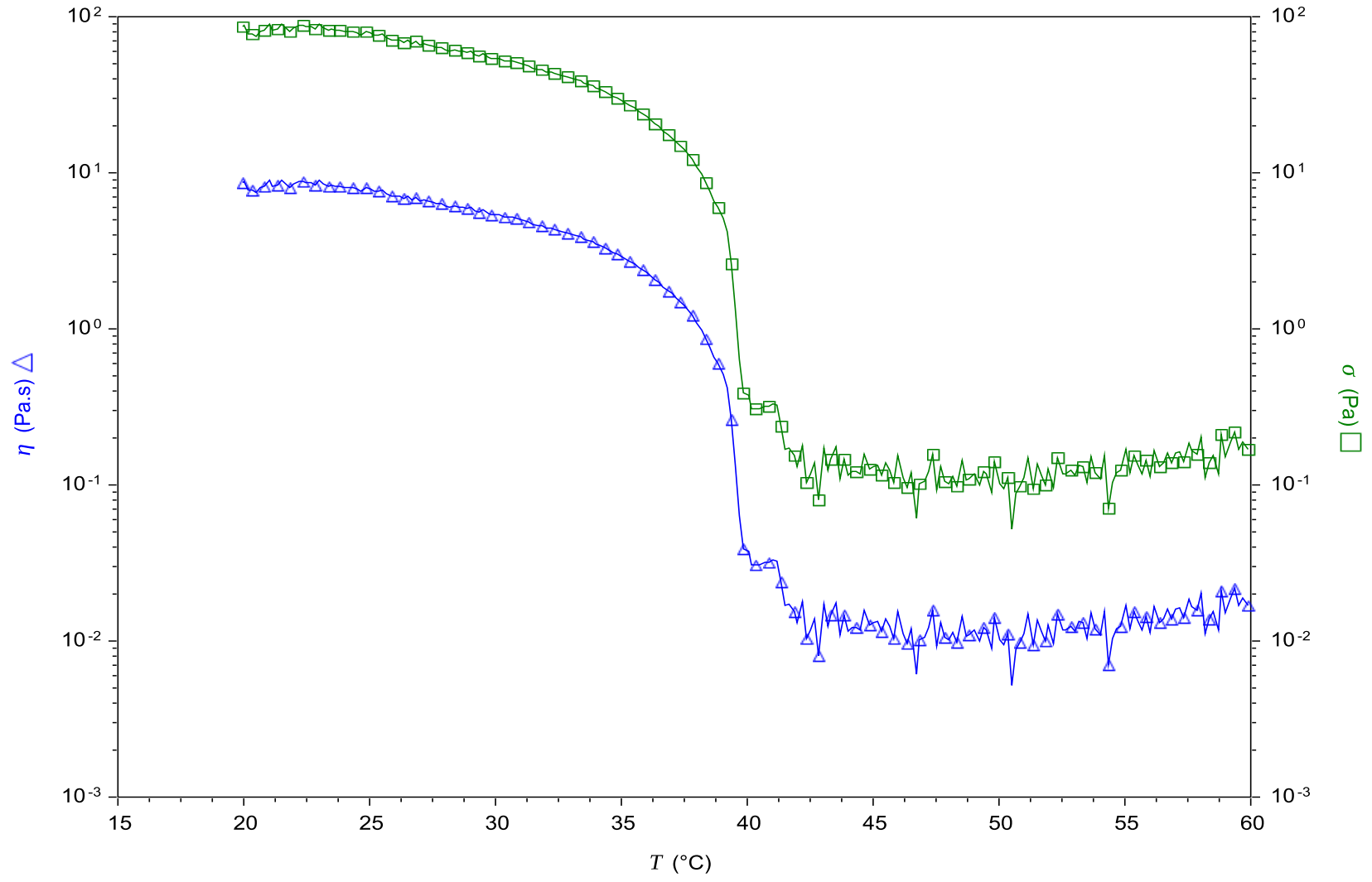
### Emulsion B



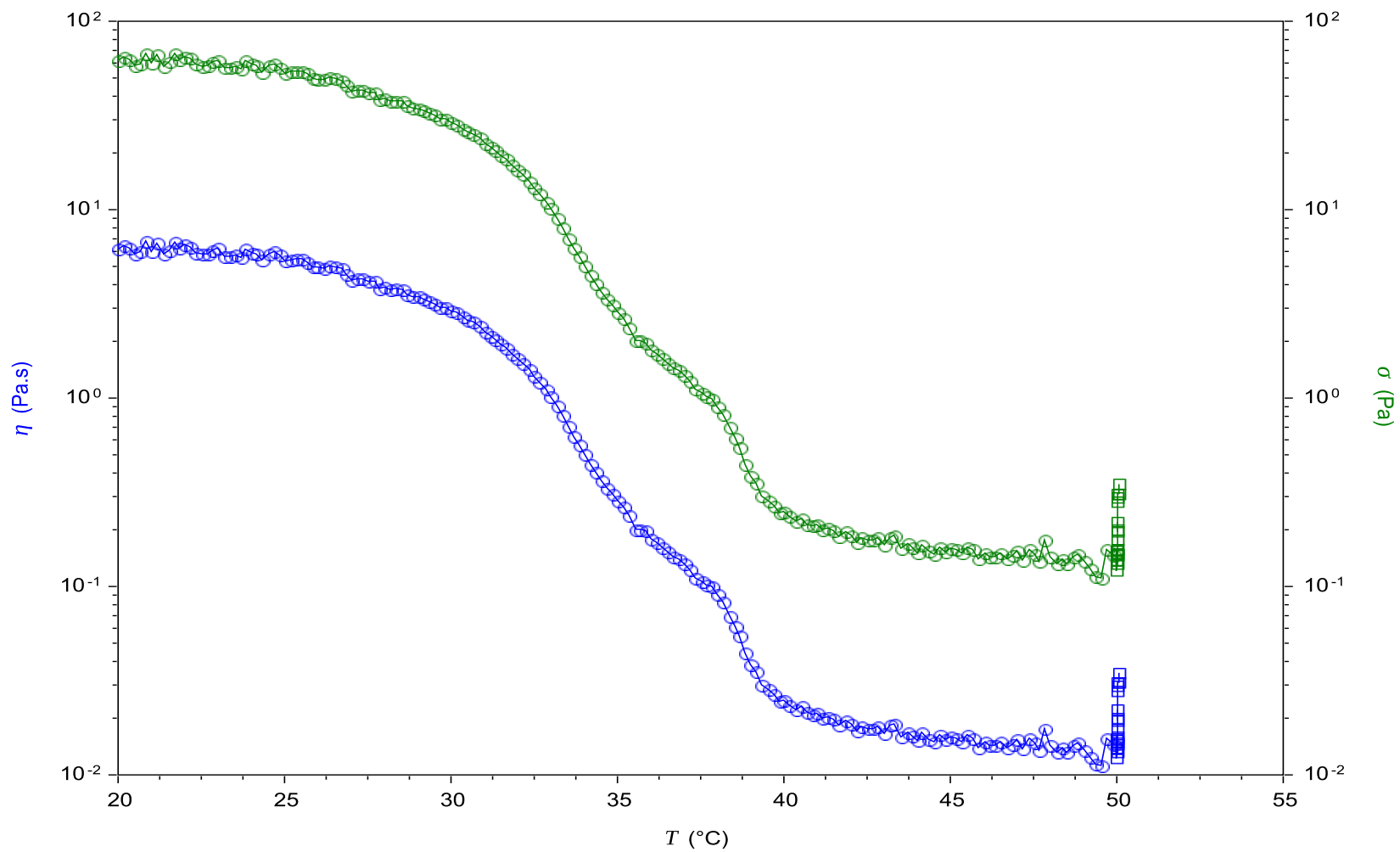
### Emulsion C



### Emulsion D



### Crude Oil A



**Appendix IV Bottle test data of Crude A experiments**

